Electronic Supplementary Material (ESI) for ChemComm.

Multiple Functional Groups in UiO-66 Improve Chemical Warfare Agent Simulant Degradation

Mark Kalaj, Joseph M. Palomba, Kyle C. Bentz, and Seth M. Cohen*

Department of Chemistry and Biochemistry, University of California, San Diego, La Jolla, California 92093, United States

SUPPORTING INFORMATION

Experimental

Materials

All solvents and starting materials were purchased from chemical suppliers and used without further purification (Sigma Aldrich, Alfa Aesar, EMD, and TCI).

Materials Synthesis

MOF Synthesis:

One Ligand Synthesis:

Zirconium(IV) chloride (0.26 mmol) and one of the following: terephthalic acid (0.26 mmol, 0.286 g), 2-aminoterephthalic acid (0.26 mmol, 0.312 g) , 2-hydroxyterephthalic acid (0.26 mmol, 0.312 g), 2-nitroterephthalic acid (0.26 mmol, 0.364 g), or 2-bromoterephthalic acid (0.26 mmol, 0.423 g) were dissolved in 15 mL DMF with 0.447 mL glacial acetic acid in a 20-mL vial. The capped vial was placed in an oven and heated to 120 °C for 24 h. After cooling to room temperature, the particles were collected by centrifugation (fixed-angle rotor, 6500 rpm, 15 min), washed with 3×10 mL portions of MeOH, and 1×10 mL hexanes and dried under vacuum at room temperature.

Two Ligand Synthesis:

Zirconium(IV) chloride (0.26 mmol) and a combination of two of the following: terephthalic acid (0.13 mmol, 0.143 g), 2-aminoterephthalic acid (0.13 mmol, 0.156 g), 2-hydroxyterephthalic acid (0.13 mmol, 0.156 g), 2-nitroterephthalic acid (0.13 mmol, 0.182 g), or 2-bromoterephthalic acid (0.13 mmol, 0.211 g) were dissolved in 15 mL DMF with 0.447 mL glacial acetic acid in a 20 mL vial. The capped vial was placed in an oven and

heated to 120 °C for 24 h. After cooling to room temperature, the particles were collected by centrifugation (fixed-angle rotor, 6500 rpm, 15 min), washed with 3×10 mL portions of MeOH, and 1×10 mL hexanes and dried under vacuum at room temperature.

Three Ligand Synthesis:

Zirconium(IV) chloride (0.26 mmol) and a combination of three of the following: terephthalic acid (0.087 mmol, 0.096 g), 2-aminoterephthalic acid (0.087 mmol, 0.105g), 2-hydroxyterephthalic acid (0.087 mmol, 0.105 g), 2-nitroterephthalic acid (0.087 mmol, 0.121 g) ,or 2-bromoterephthalic acid (0.087 mmol, 0.141 g) were dissolved in 15 mL DMF with 0.447 mL glacial acetic acid in a 20 mL vial. The capped vial was placed in an oven and heated to 120 °C for 24 h. After cooling to room temperature, the particles were collected by centrifugation (fixed-angle rotor, 6500 rpm, 15 min), washed with 3×10 mL portions of MeOH, and 1×10 mL hexanes and dried under vacuum at room temperature.

Four Ligand Synthesis:

Zirconium(IV) chloride (0.26 mmol) and a combination of four of the following: terephthalic acid (0.065 mmol, 0.072 g), 2-aminoterephthalic acid (0.065 mmol, 0.078 g), 2-hydroxyterephthalic acid (0.065 mmol, 0.078 g), 2-nitroterephthalic acid (0.065 mmol, 0.091 g), or 2-bromoterephthalic acid (0.065 mmol, 0.106 g) were dissolved in 15 mL DMF with 0.447 mL glacial acetic acid in a 20 mL vial. The capped vial was placed in an oven and heated to 120 °C for 24 h. After cooling to room temperature, the particles were collected by centrifugation (fixed-angle rotor, 6500 rpm, 15 min), washed with 3×10 mL portions of MeOH, and 1×10 mL hexanes and dried under vacuum at room temperature.

Five Ligand Synthesis:

Zirconium(IV) chloride (0.26 mmol) and terephthalic acid (0.052 mmol, 0.057 g), 2-aminoterephthalic acid (0.052 mmol, 0.062 g), 2-hydroxyterephthalic acid (0.052 mmol, 0.062 g), 2-nitroterephthalic acid (0.052 mmol, 0.073 g), or 2-bromoterephthalic acid (0.052 mmol, 0.085 g) were dissolved in 15 mL DMF with 0.447 mL glacial acetic acid in a 20 mL vial. The capped vial was placed in an oven and heated to 120 °C for 24 h. After cooling to room temperature, the particles were collected by centrifugation (fixed-angle rotor, 6500 rpm, 15 min), washed with 3×10 mL portions of MeOH, and 1×10 mL hexanes and dried under vacuum at room temperature.

Characterization Methods

Nuclear Magnetic Resonance (NMR). Proton nuclear magnetic resonance spectra (^{1}H NMR) were recorded on a Varian FT-NMR spectrometer (400 MHz). Chemical shifts are quoted in parts per million (ppm) referenced to the appropriate solvent peak or 0 ppm for TMS. MOFs were digested for NMR analysis by immersion of ~8-10 mg MOF in 580 μL DMSO-d_6 with 20 μL HF (48% in water). Samples were kept in this acidic solution at room temperature until the MOF was fully dissolved.

Powder X-ray Diffraction (PXRD). PXRD data was collected at room temperature on a Bruker D8 Advance diffractometer running at 40 kV, 40 mA for Cu Kα (λ = 1.5418 Å), with a scan speed of 0.5 sec/step, a step size of 0.01° in 2θ, and a 2θ range of 3-50° at room temperature.

Scanning Electron Microscopy (SEM). MOFs were placed on conductive carbon tape on a sample holder and coated using an Ir-sputter coating for 7 sec. A Zeiss Sigma 500 ESEM microscope was used for acquiring images using a 2-3 kV energy source under vacuum at a working distance of 5 mm.

Thermogravimetric analysis (TGA). ~10 mg of sample were placed in a 100 μL aluminum crucible. Samples were analyzed on a Mettler Toledo Star TGA/DSC using a temperature range of 30-600 °C scanning at 5 °C/min synthetic air (75 cm^3/min air flow rate) for sample degradation measurements and a heat-cool-heat procedure at 10 °C/min for melting point determination.

N_2 Gas Sorption Analysis: Samples for analysis were evacuated in a vacuum oven overnight at room temperature prior to analysis. ~50 mg of sample were then transferred to pre-weighed sample tubes and degassed at 105° C on a Micromeritics ASAP 2020 Adsorption Analyzer for a minimum of 12 h or until the outgas rate was <5 mmHG. After degassing, the sample tubes were re-weighed to obtain a consistent mass for the samples. Sorption data and BET surface area (m^2/g) measurements were collected at 77 K with N_2 on a Micromeritics ASAP 2020 Adsorption Analyzer using volumetric technique.

Catalysis Experiments. In this study, DMNP hydrolysis was measured using a modified version of a previously reported procedure (*Chem. Commun.* **2018**, *54*, 5768-5771). All catalytic monitoring was carried out using a BioTek Synergy H4 plate reader using single wavelength absorbance mode. 20 and 40 mM of *N*-ethylmorpholine buffer was prepared

from deionized water adjusted to pH = 8.0. A plot of absorbance of *p*-nitrophenol at varying concentrations was measured yielding a calibration curve with a slope of 3.48 Abs/mM (*Chem. Commun.* **2018**, *54*, 5768-5771). MOF samples were prepared by weighing 6 mg of MOF powder and diluting this powder in 10 mL of deionized water. These solutions were rigorously sonicated and vortexed (>3× of each) and diluted in half with 40 mM buffer solution yielding 300 μg/mL MOF in 20 mM buffer solution. Dimethyl *p*-nitrophenylphosphate (DMNP) hydrolysis assays with MOF powders were carried out in Olympus Plastics clear, flat-bottom 96-well plates. Each well was prepared with 100 μL total volume containing: 95 μL MOF suspension in buffer and 5 μL substrate (25 mM DMNP in MeOH; 1.25 mM total concentration; 0.125 μmol). Upon the addition of substrate using a multi-channel pipette, hydrolysis was monitored by the change in absorbance (λ_{max} = 407 nm) over 15 min at 24 °C with 3 sec shaking of the plate every 10 sec. The absorbance was monitored from the 30 to 360 sec time period, as previously reported (*Chem. Commun.* **2019**, *55*, 3481-3484). Reported activities for MOF samples are an average of seven replicates. Hydrolysis rates were adjusted to account for the increased mass of the various species such that a direct comparison could be made across all materials in this study as previously reported (*Chem. Commun.* **2019**, *55*, 3481-3484).

Characterization

Powder X-ray Diffraction (PXRD) and ^{1}H NMR Digestions

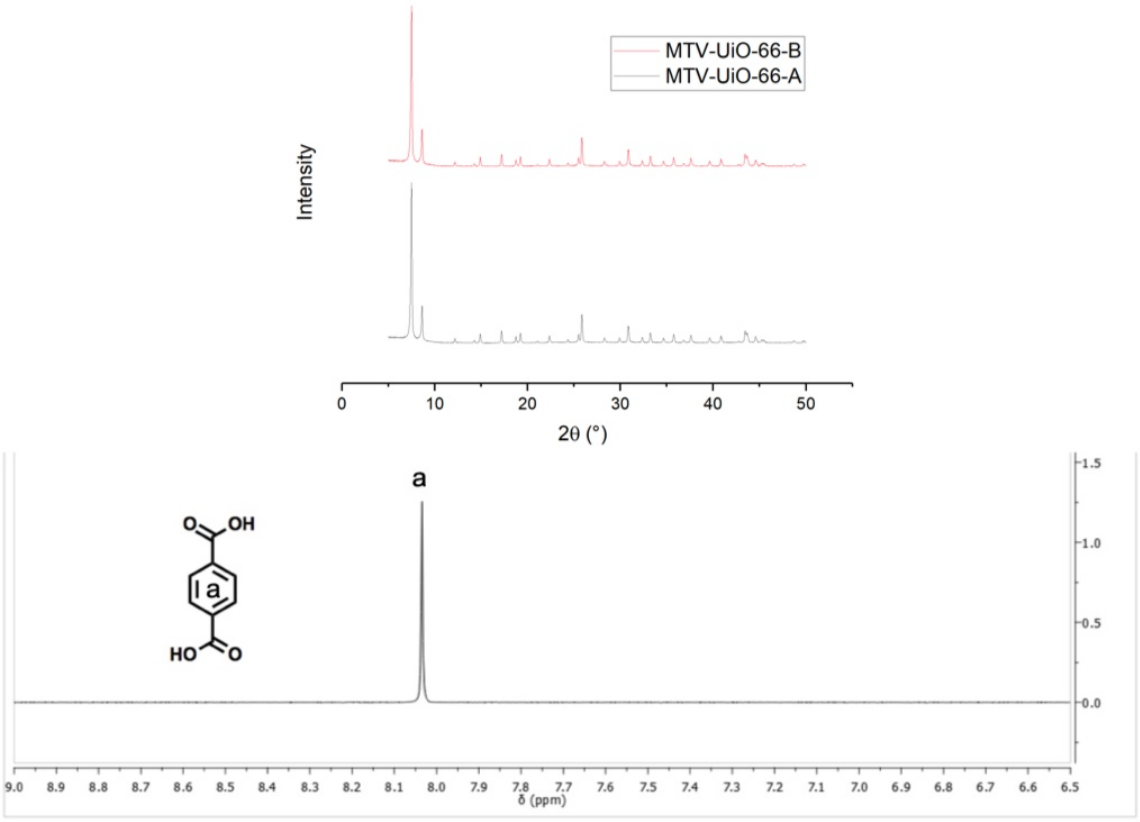

Figure S1. *Top*: PXRD of MTV-UiO-66-A. *Bottom*: ^{1}H NMR digestion of MTV-UiO-66-A.

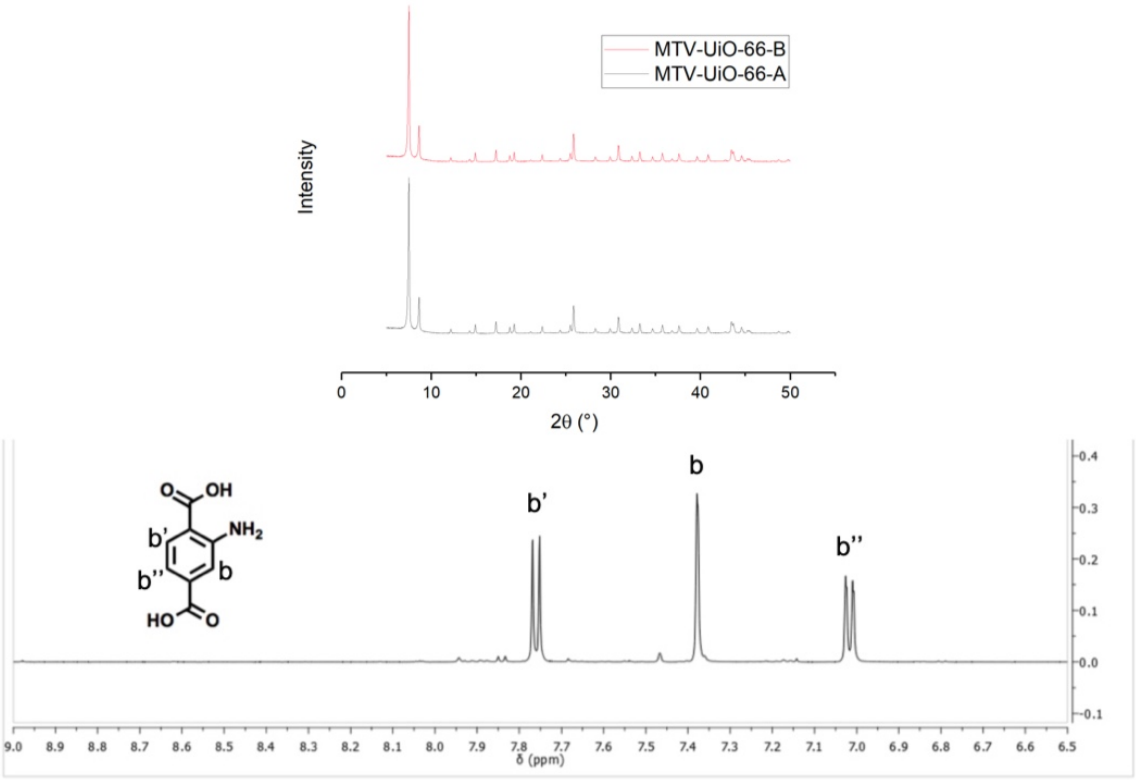

Figure 2. *Top*: PXRD of MTV-UiO-66-B. *Bottom*: ^{1}H NMR digestion of MTV-UiO-66-B.

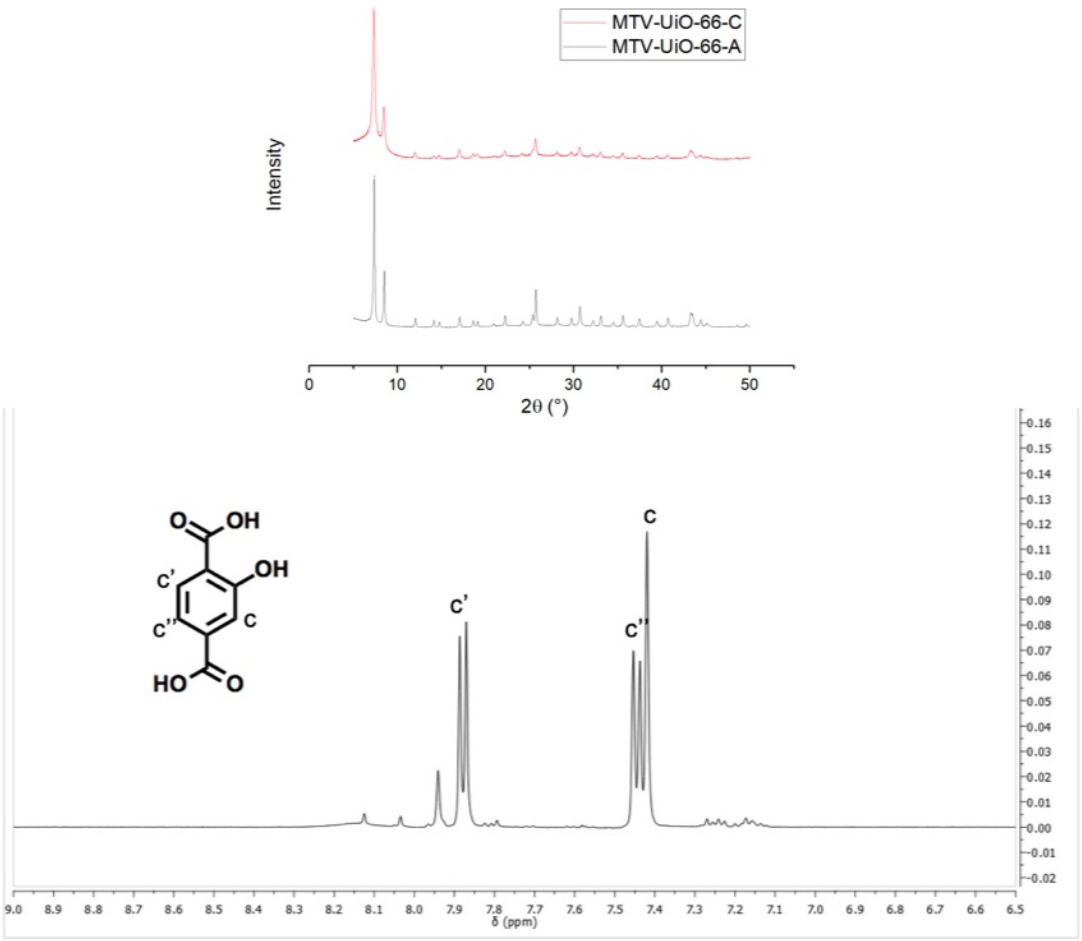

Figure S3. *Top*: PXRD of MTV-UiO-66-C. *Bottom*: ^{1}H NMR digestion of MTV-UiO-66-C.

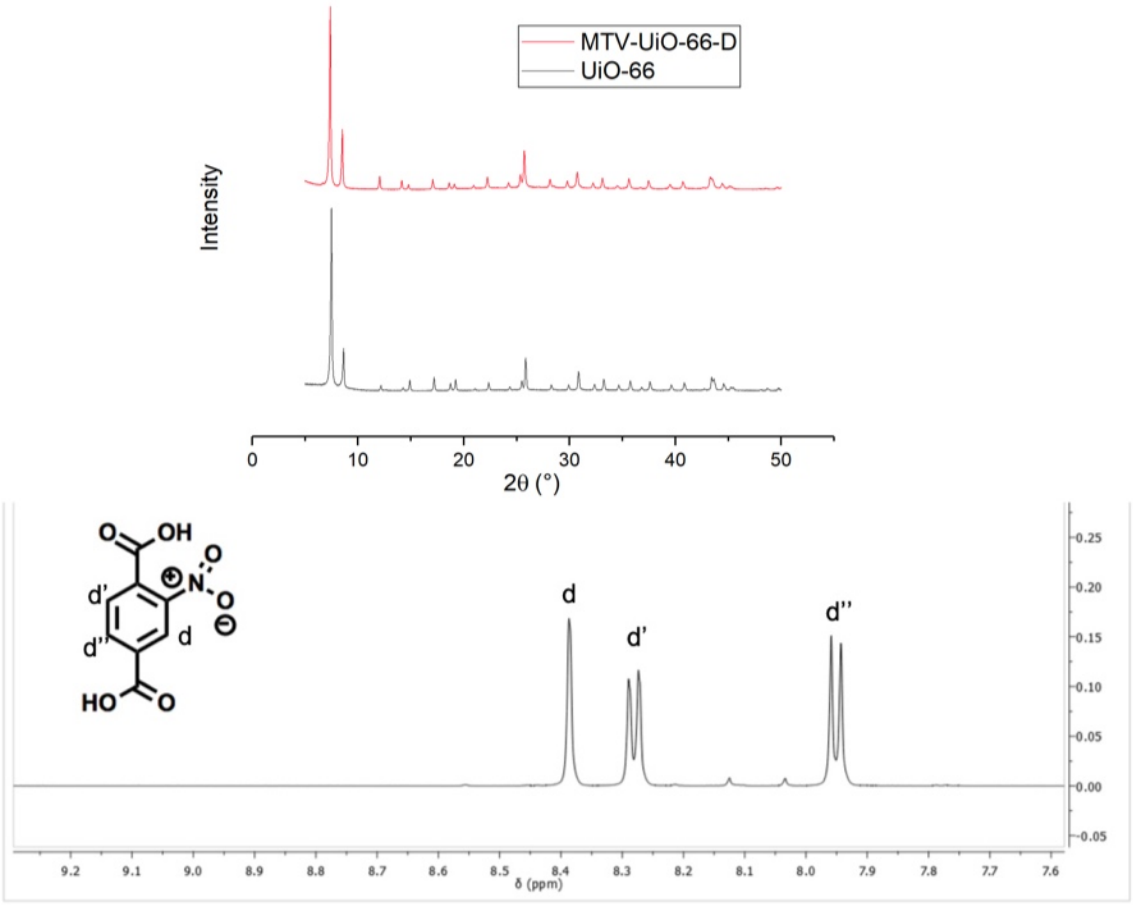

Figure S4. *Top*: PXRD of MTV-UiO-66-D. *Bottom*: ^{1}H NMR digestion of MTV-UiO-66-D.

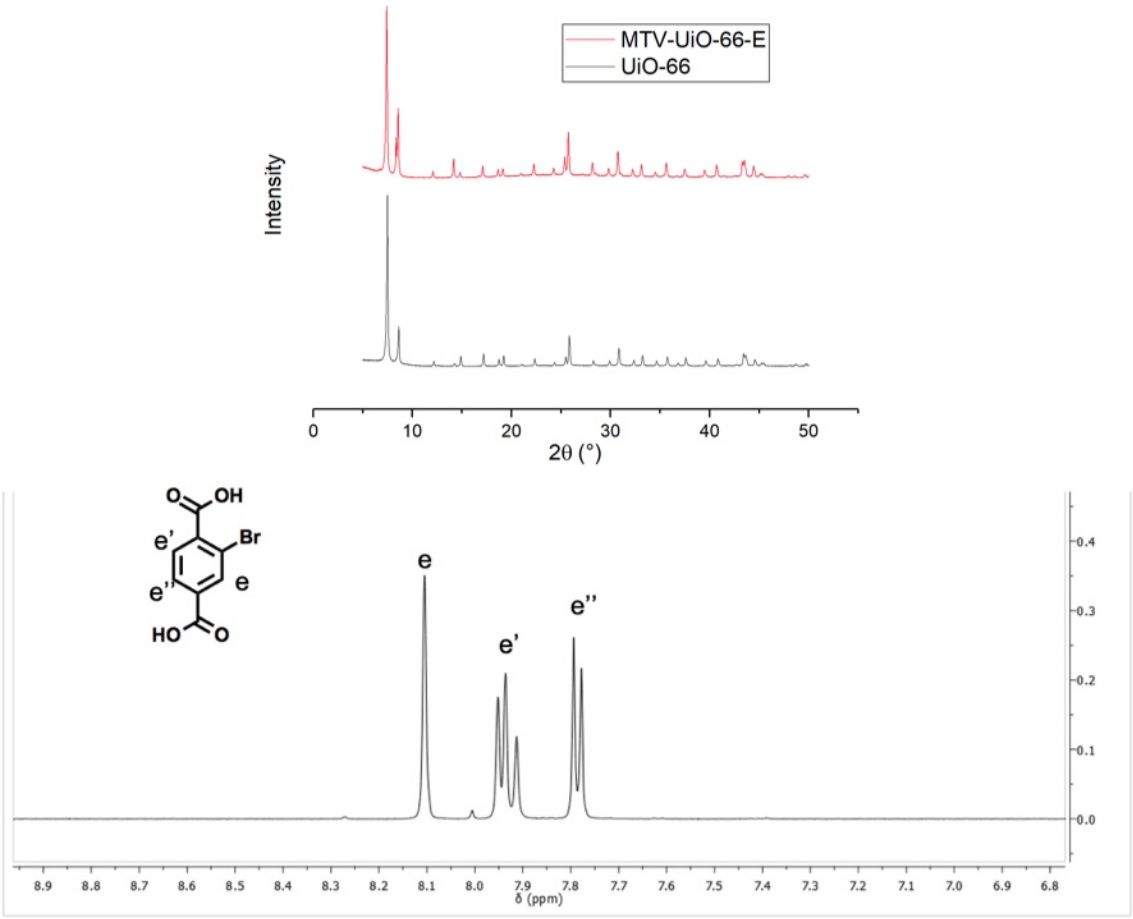

Figure S5. *Top*: PXRD of MTV-UiO-66-E. *Bottom*: ^{1}H NMR digestion of MTV-UiO-66-E.

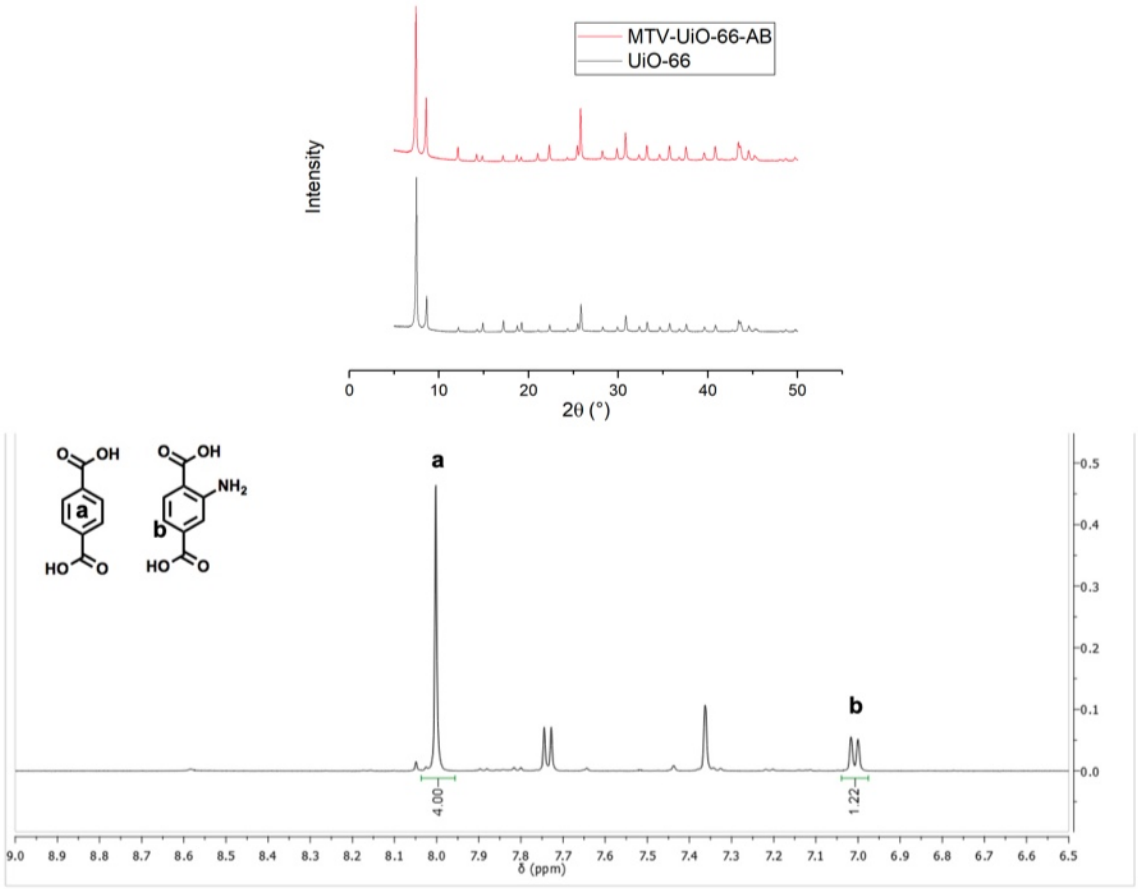

Figure S6. *Top*: PXRD of MTV-UiO-66-AB. *Bottom*: ^{1}H NMR digestion of MTV-UiO-66-AB.

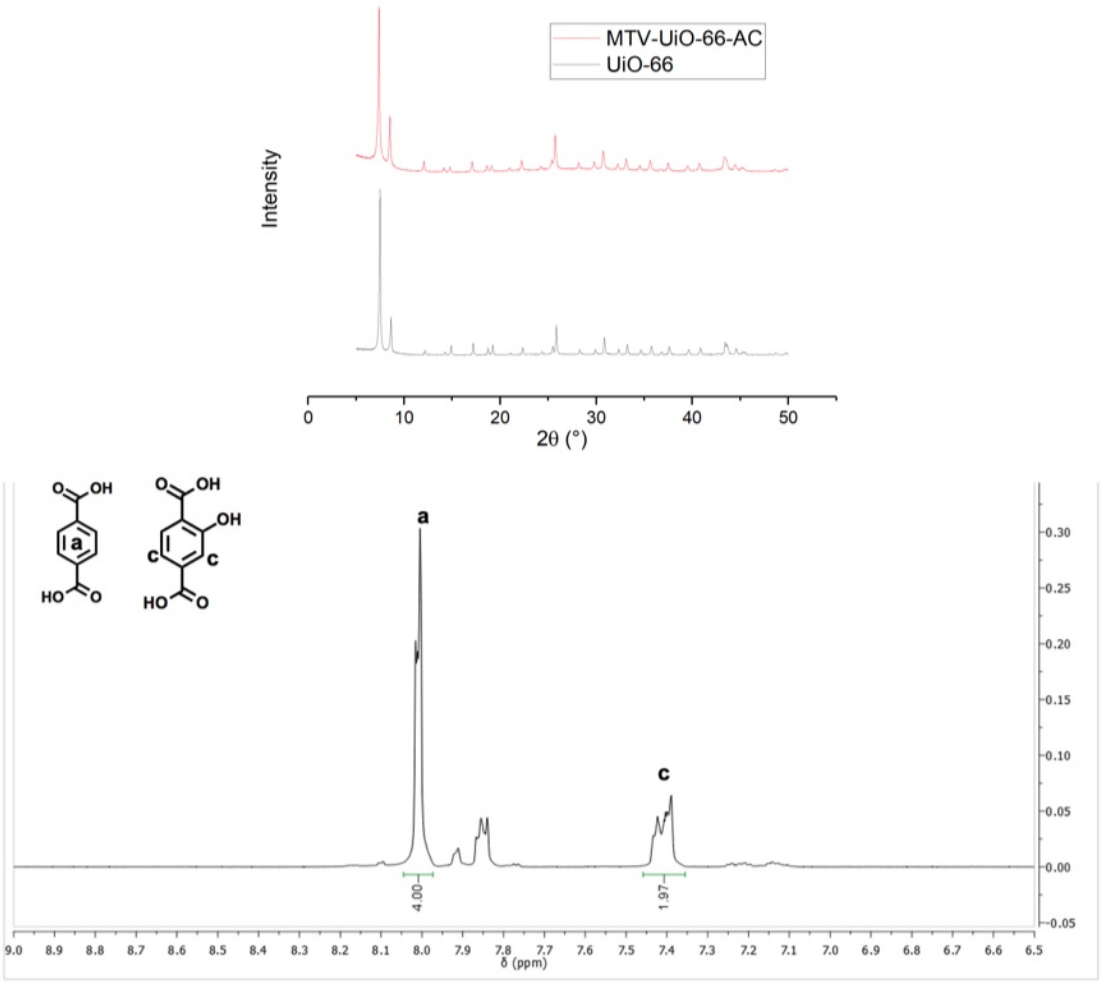

Figure S7. *Top*: PXRD and SEM of MTV-UiO-66-AC. *Bottom*: ^{1}H NMR digestion of MTV-UiO-66-AC.

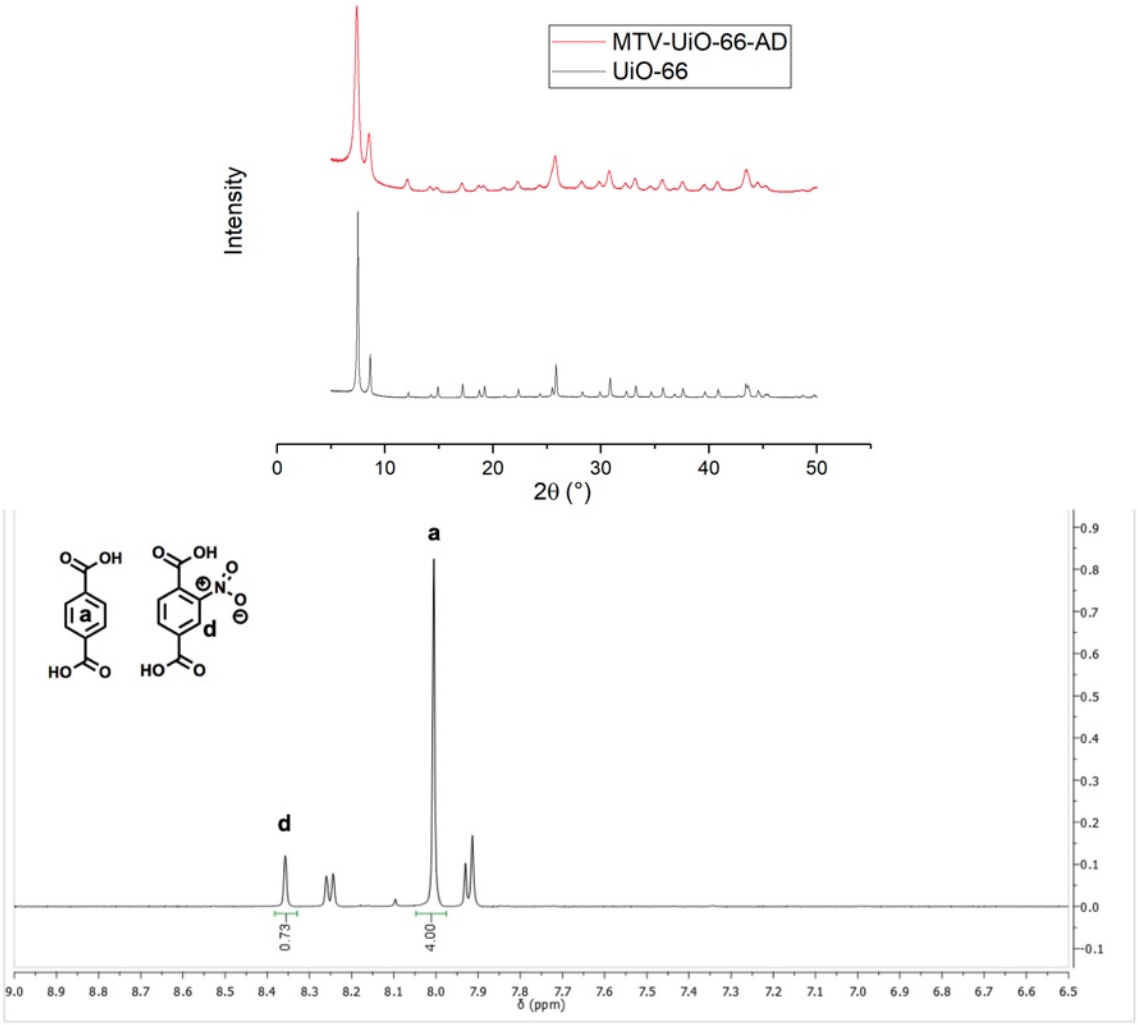

Figure S8. *Top*: PXRD of MTV-UiO-66-AD. *Bottom*: ^{1}H NMR digestion of MTV-UiO-66-AD.

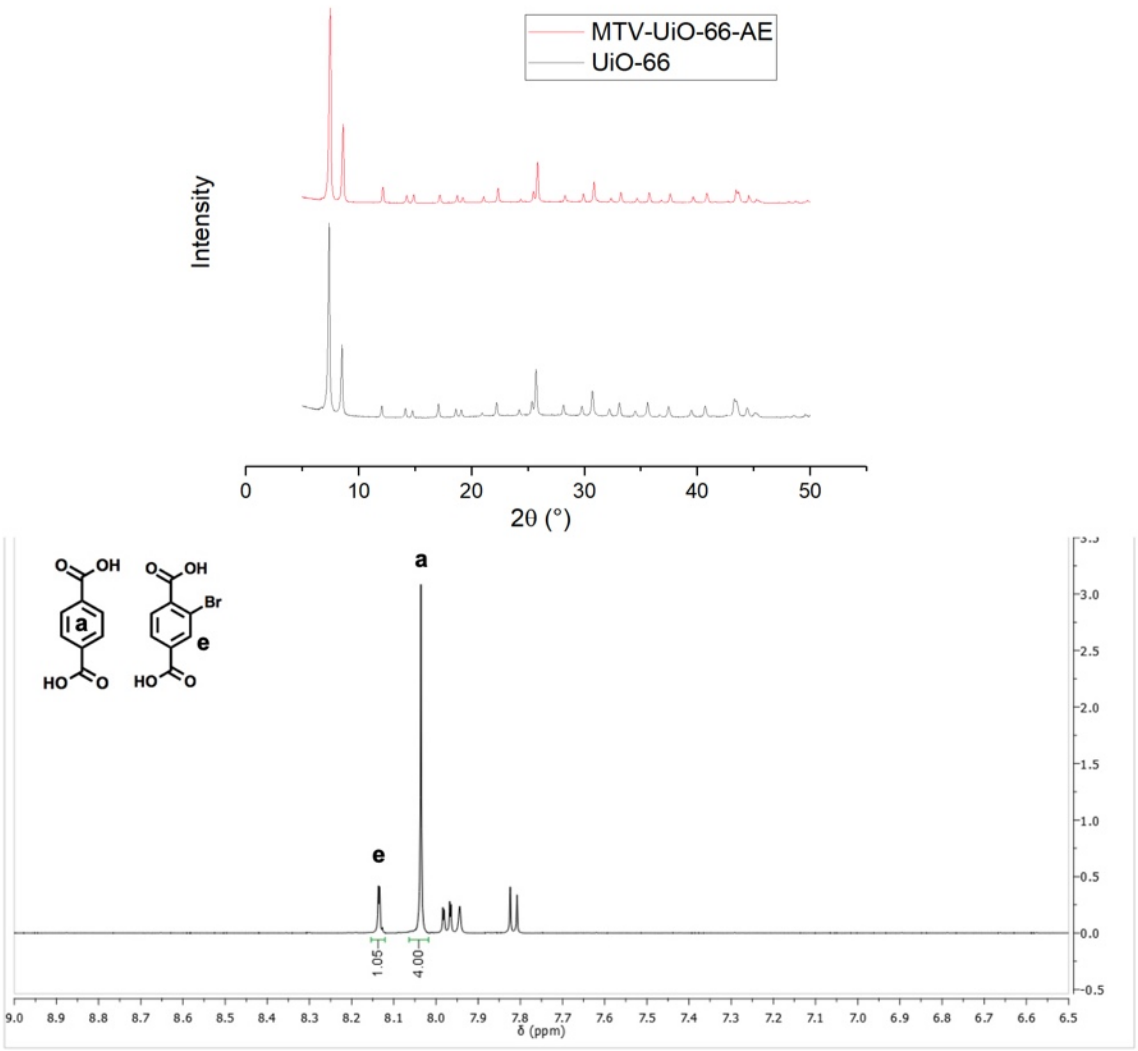

Figure S9. *Top*: PXRD of MTV-UiO-66-AE. *Bottom*: ^{1}H NMR digestion of MTV-UiO-66-AE.

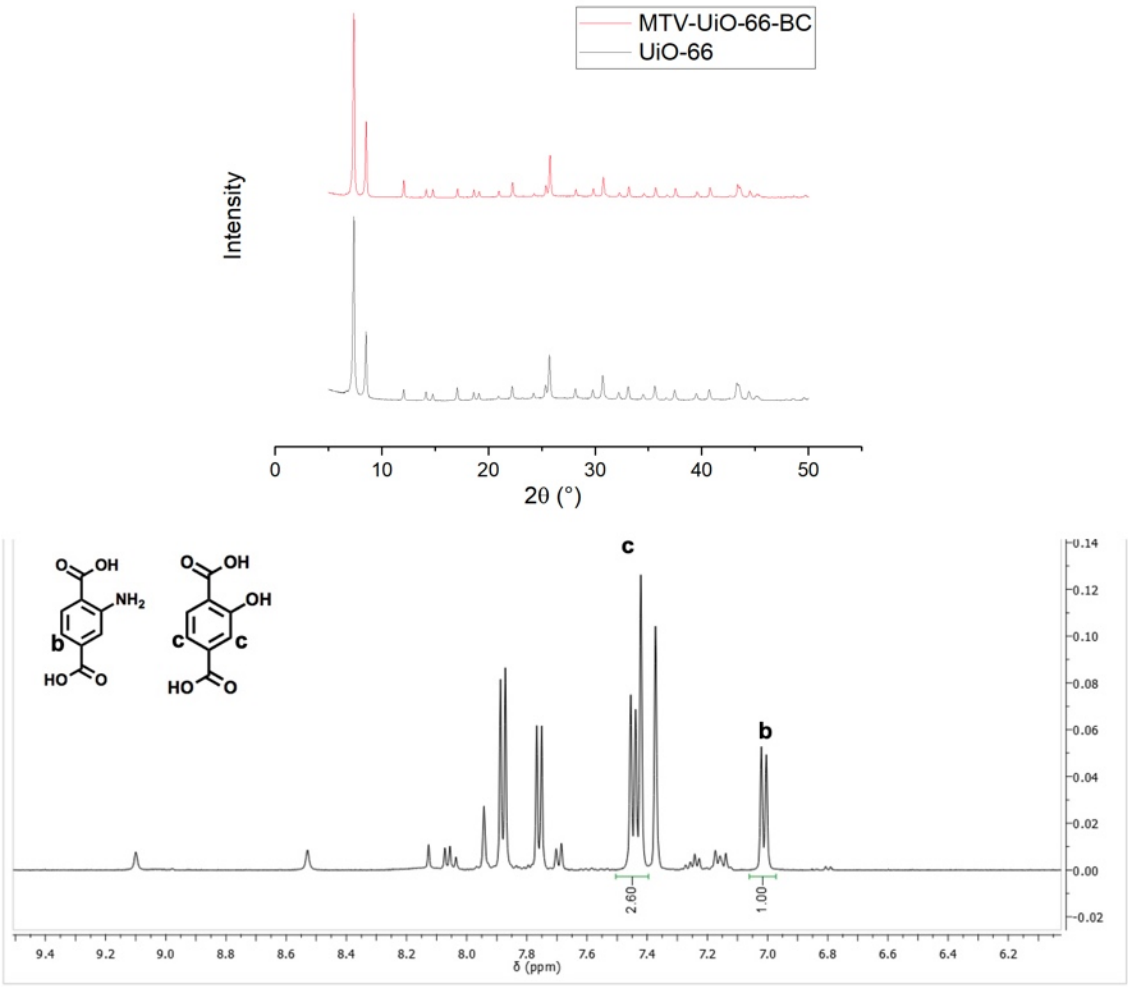

Figure S10. *Top*: PXRD of MTV-UiO-66-BC. *Bottom*: ^{1}H NMR digestion of MTV-UiO-66-BC.

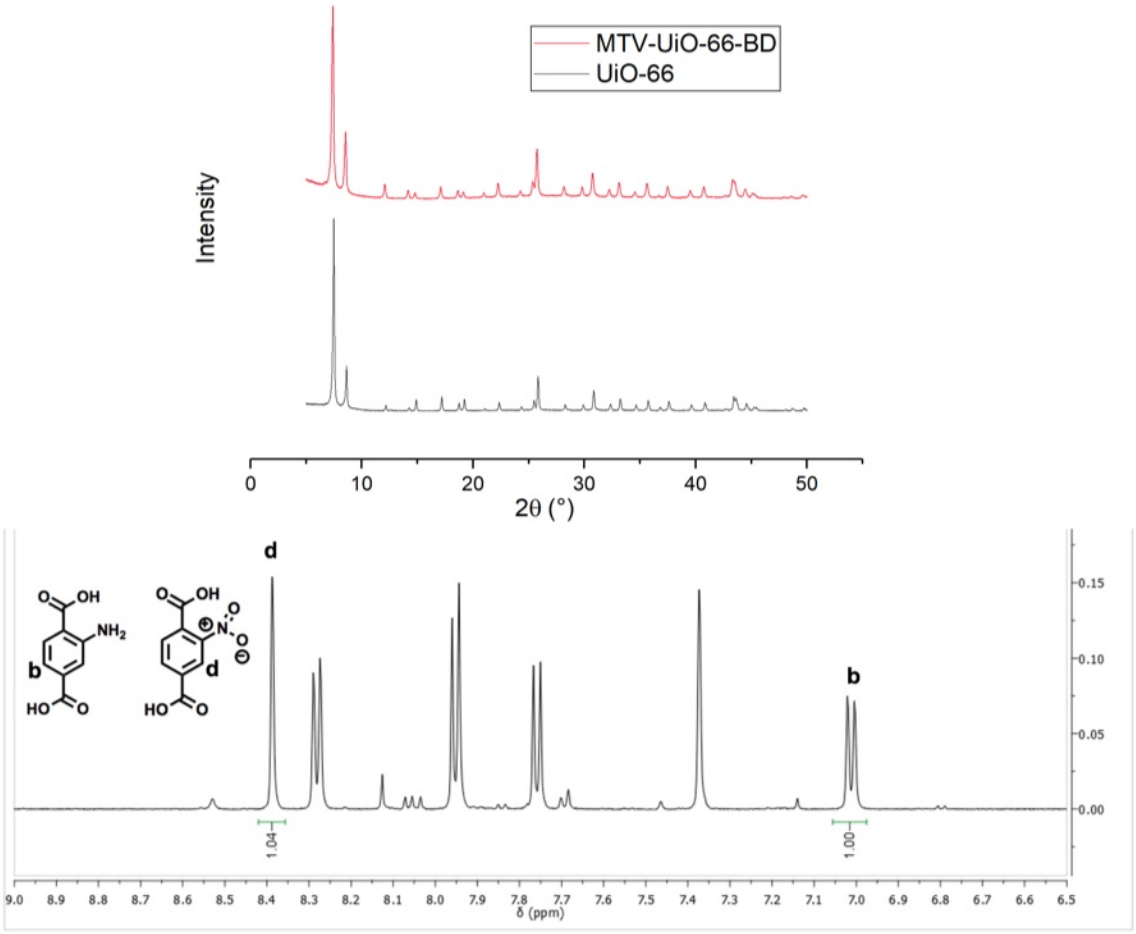

Figure S11. *Top*: PXRD of MTV-UiO-66-BD. *Bottom*: ^{1}H NMR digestion of MTV-UiO-66-BD.

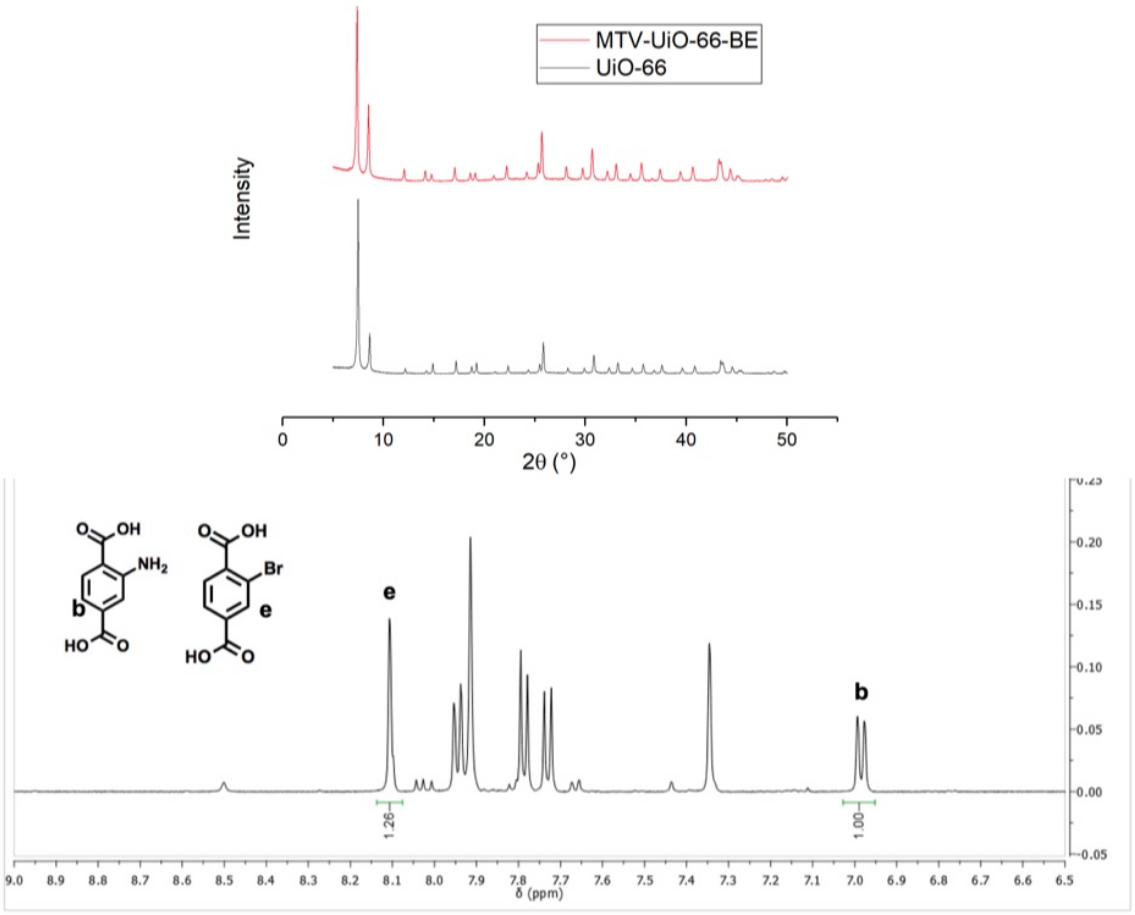

Figure S12. *Top*: PXRD of MTV-UiO-66-BE. *Bottom*: ^{1}H NMR digestion of MTV-UiO-66-BE.

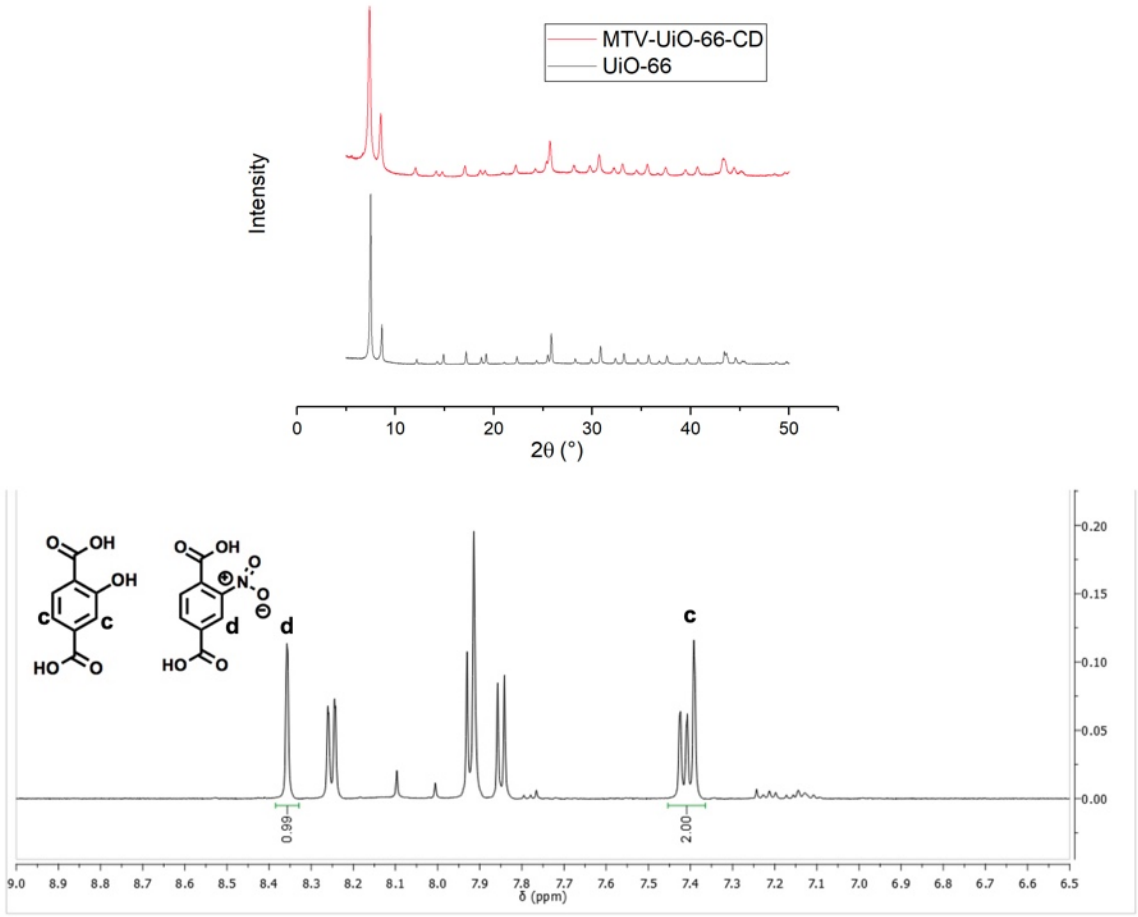

Figure S13. *Top*: PXRD of MTV-UiO-66-CD. *Bottom*: ^{1}H NMR digestion of MTV-UiO-66-CD.

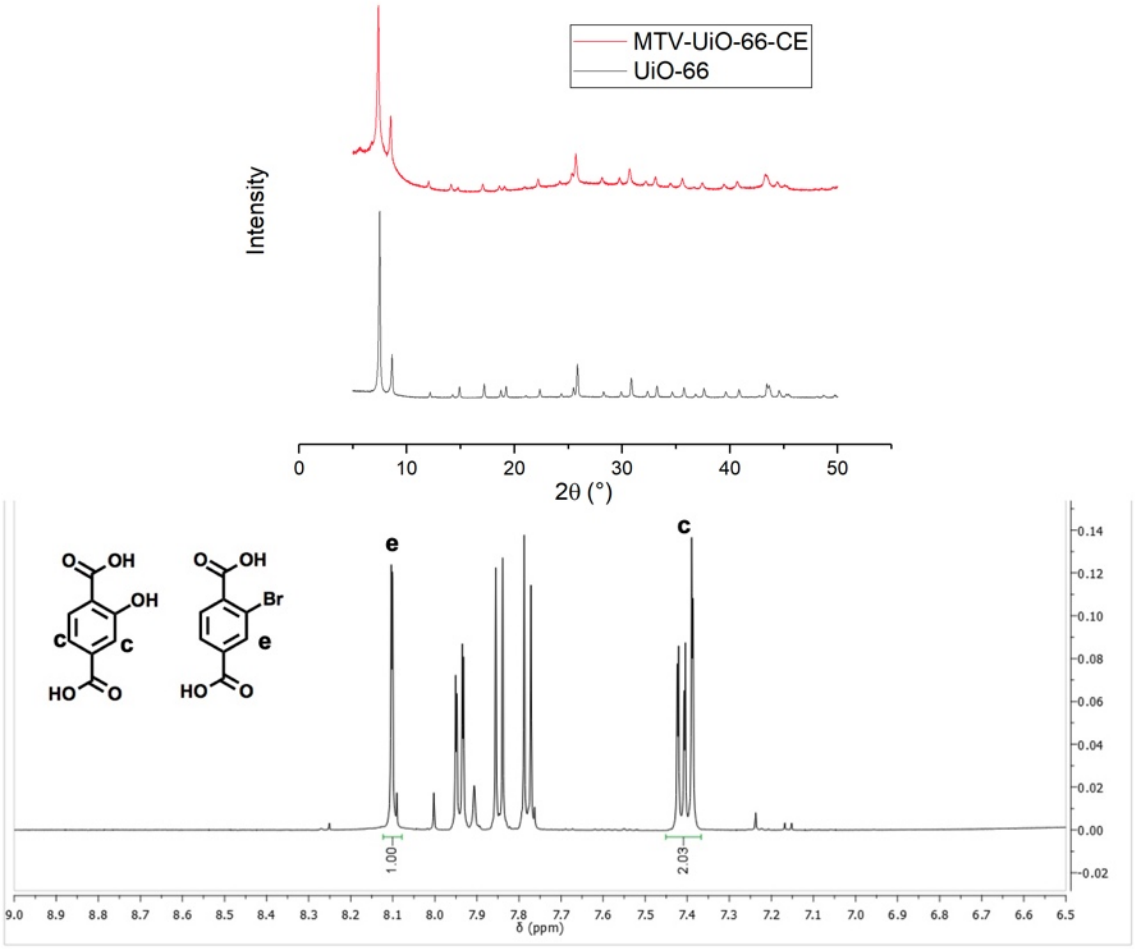

Figure S14. *Top*: PXRD of MTV-UiO-66-CE. *Bottom*: ^{1}H NMR digestion of MTV-UiO-66-CE.

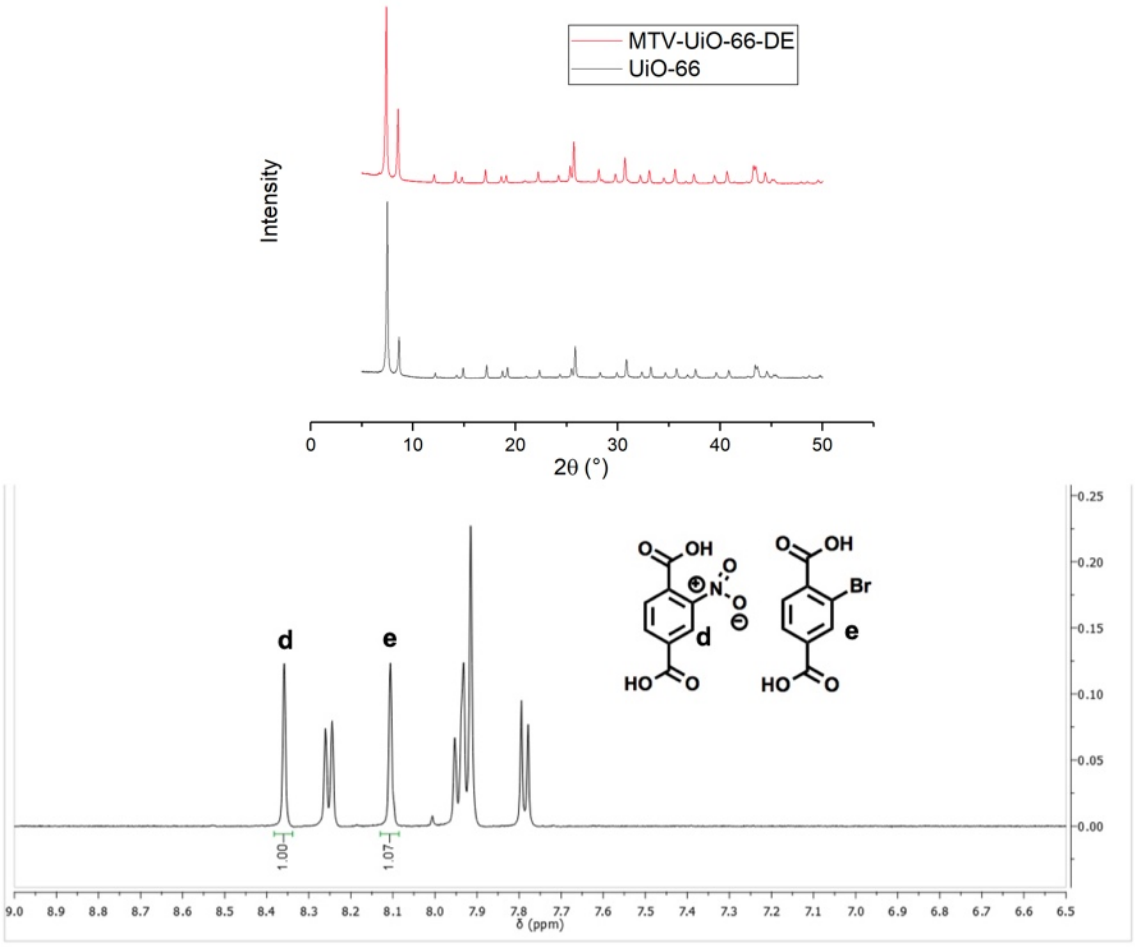

Figure S15. *Top*: PXRD of MTV-UiO-66-DE. *Bottom*: ^{1}H NMR digestion of MTV-UiO-66-DE.

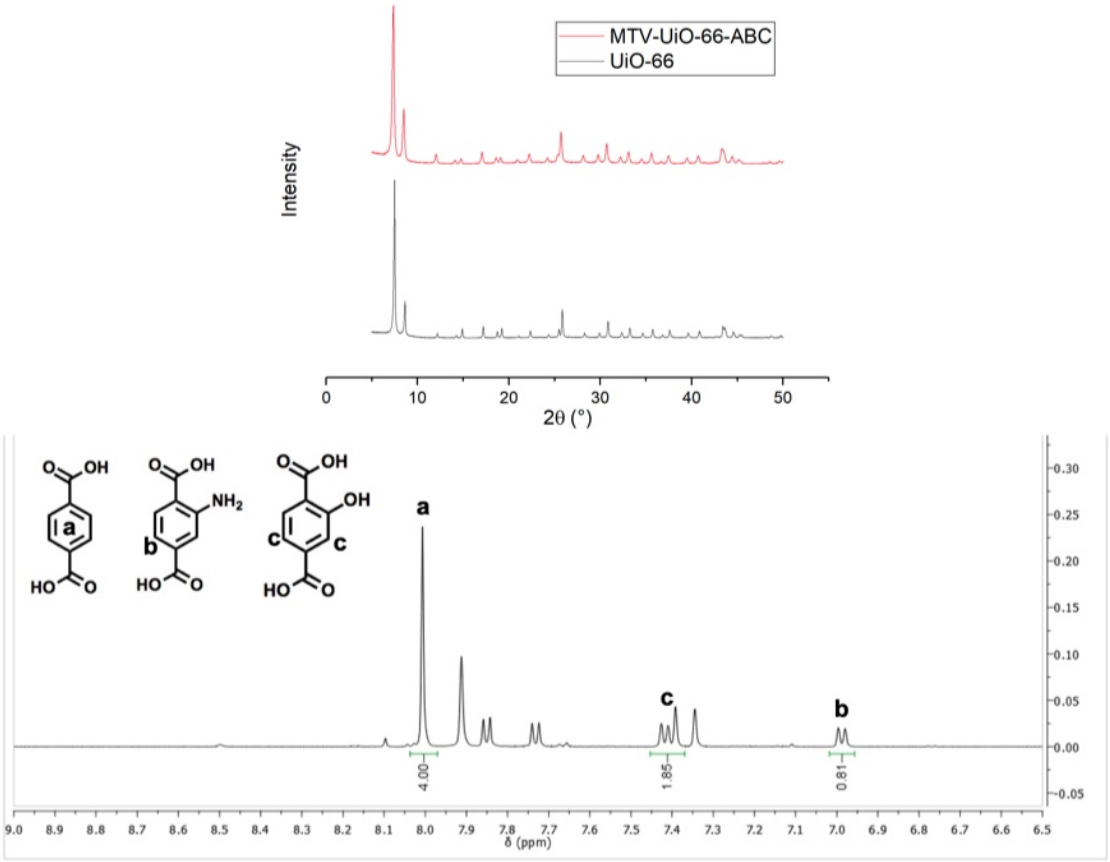

Figure S16. *Top*: PXRD of MTV-UiO-66-ABC. *Bottom*: ^{1}H NMR digestion of MTV-UiO-66-ABC.

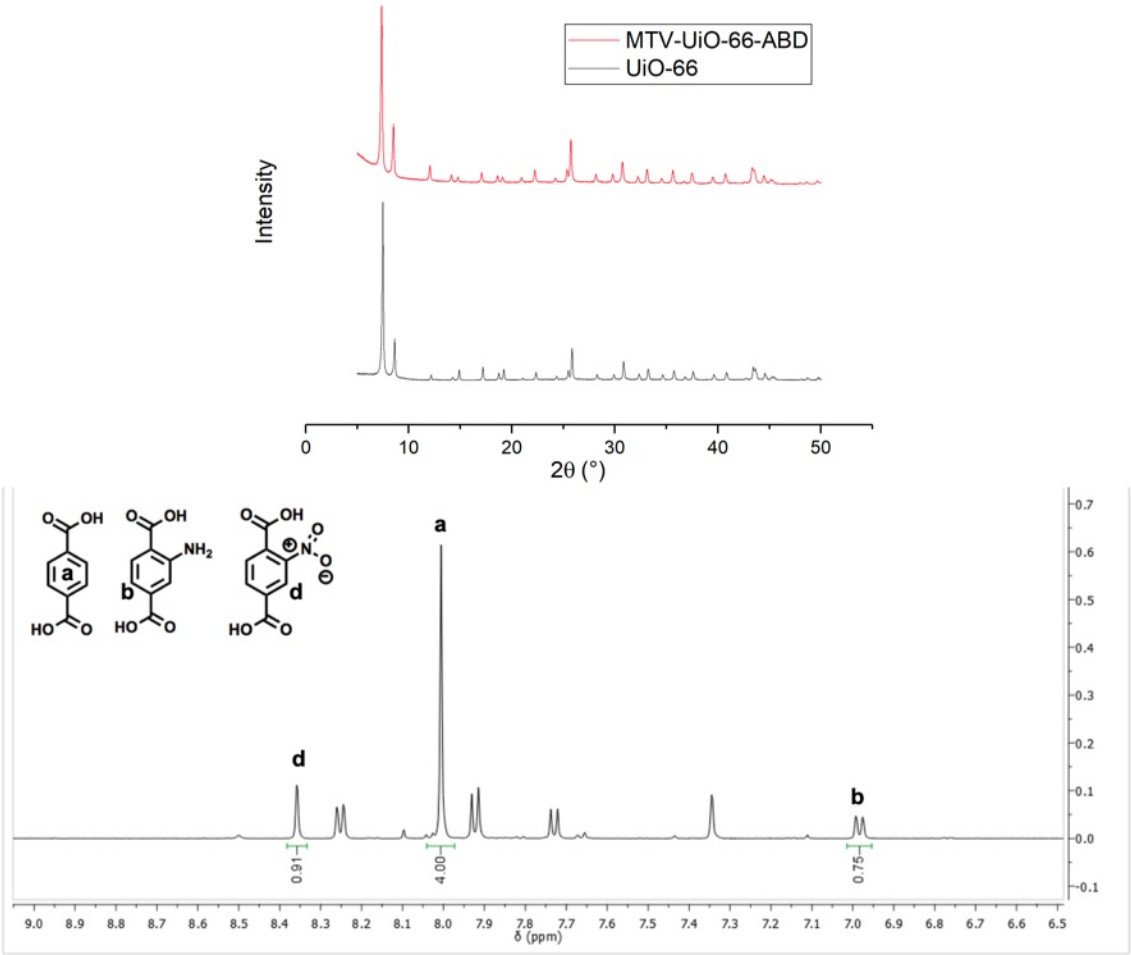

Figure S17. *Top*: PXRD of MTV-UiO-66-ABD. *Bottom*: ^{1}H NMR digestion of MTV-UiO-66-ABD.

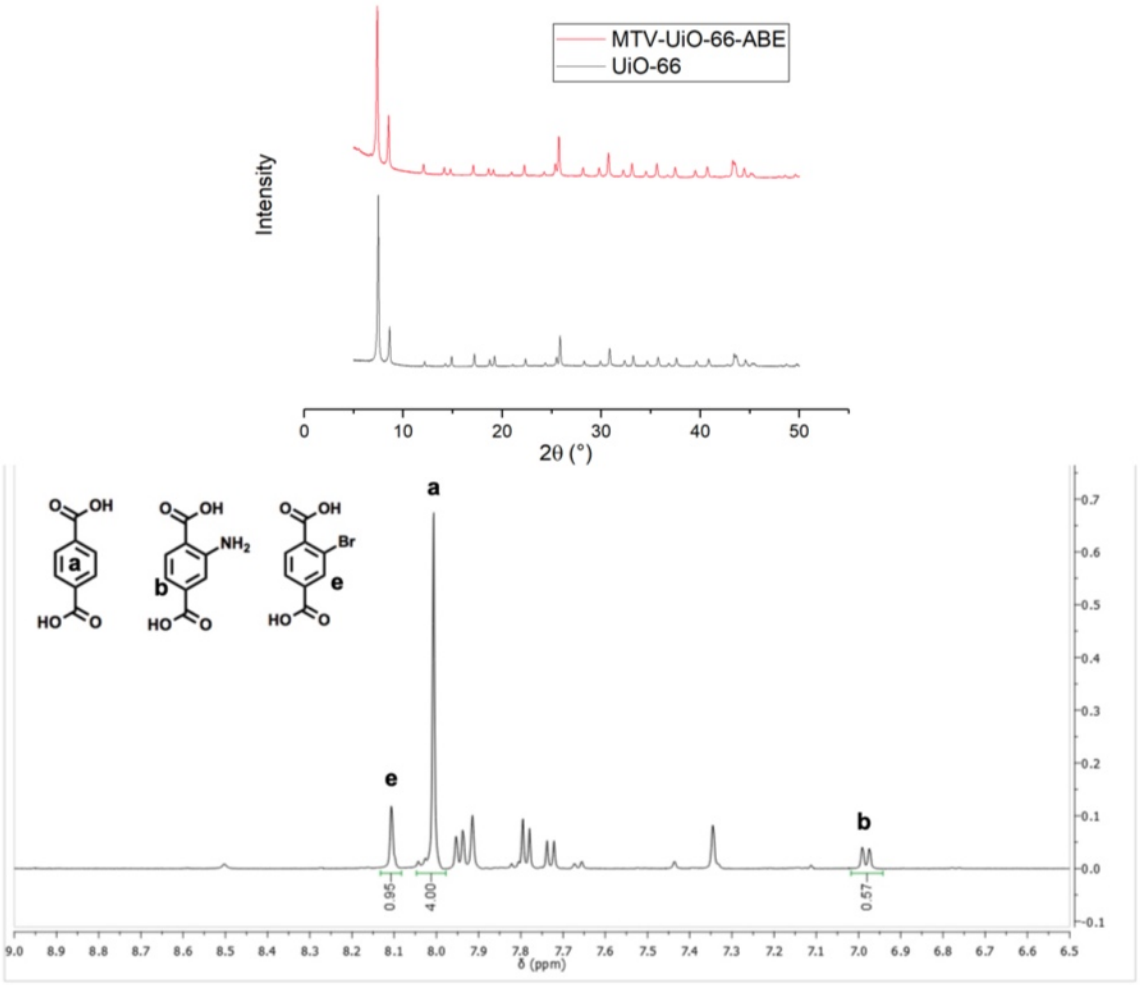

Figure S18. *Top*: PXRD of MTV-UiO-66-ABE. *Bottom*: ^{1}H NMR digestion of MTV-UiO-66-ABE.

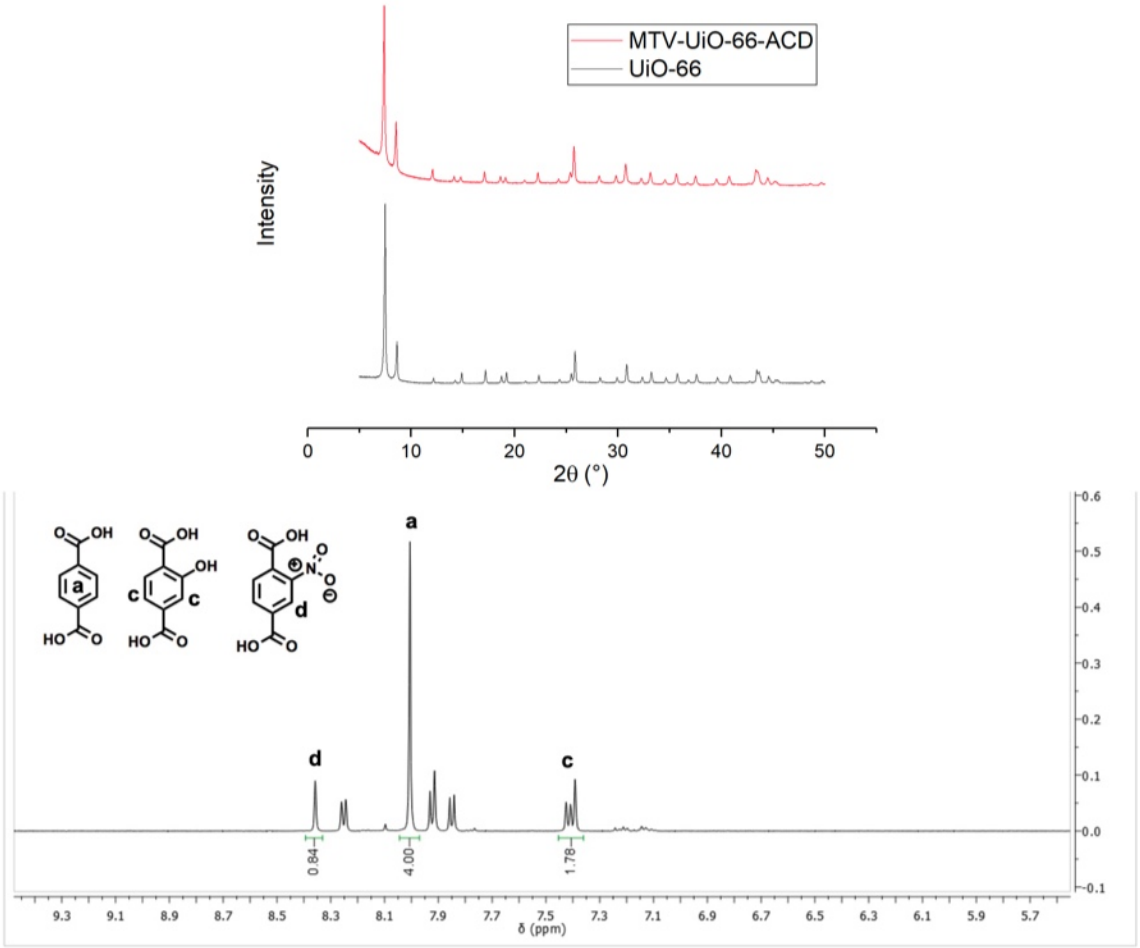

Figure S19. *Top*: PXRD of MTV-UiO-66-ACD. *Bottom*: ^{1}H NMR digestion of MTV-UiO-66-ACD.

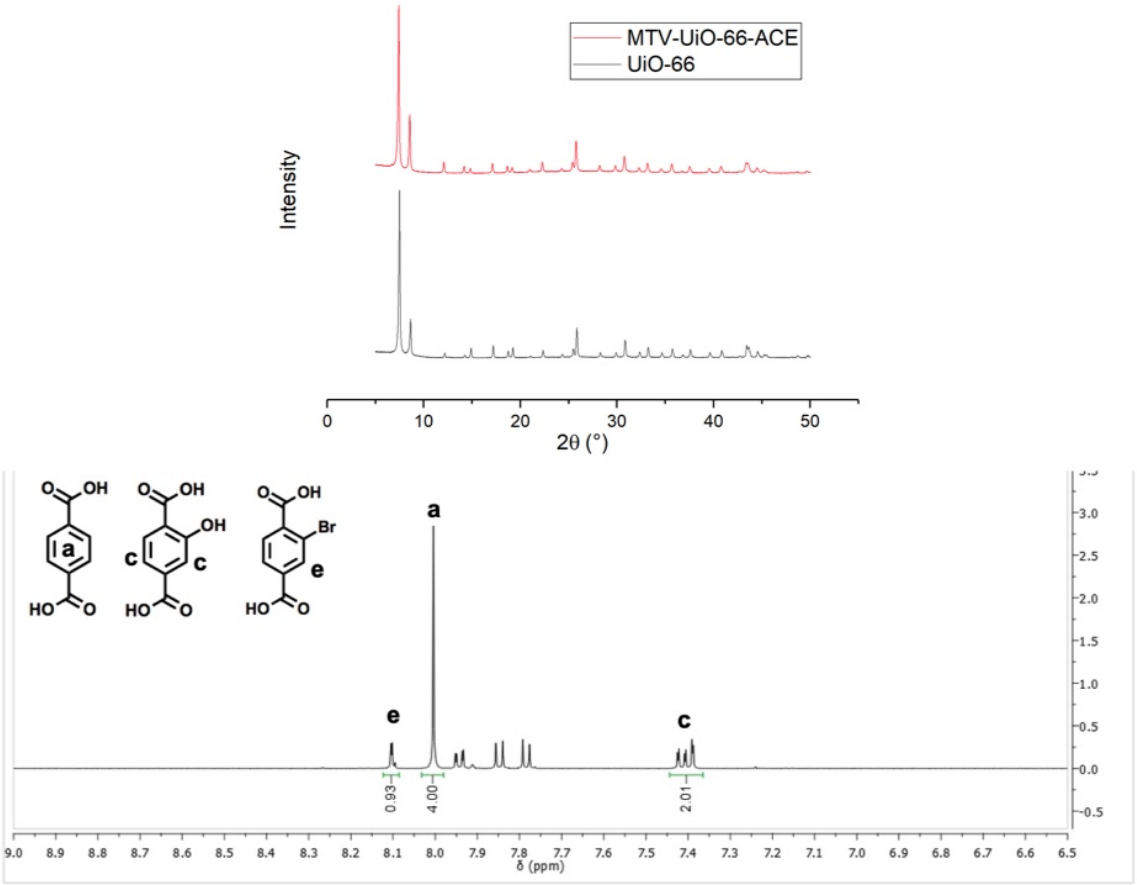

Figure S20. *Top*: PXRD of MTV-UiO-66-ACE. *Bottom*: ^{1}H NMR digestion of MTV-UiO-66-ACE.

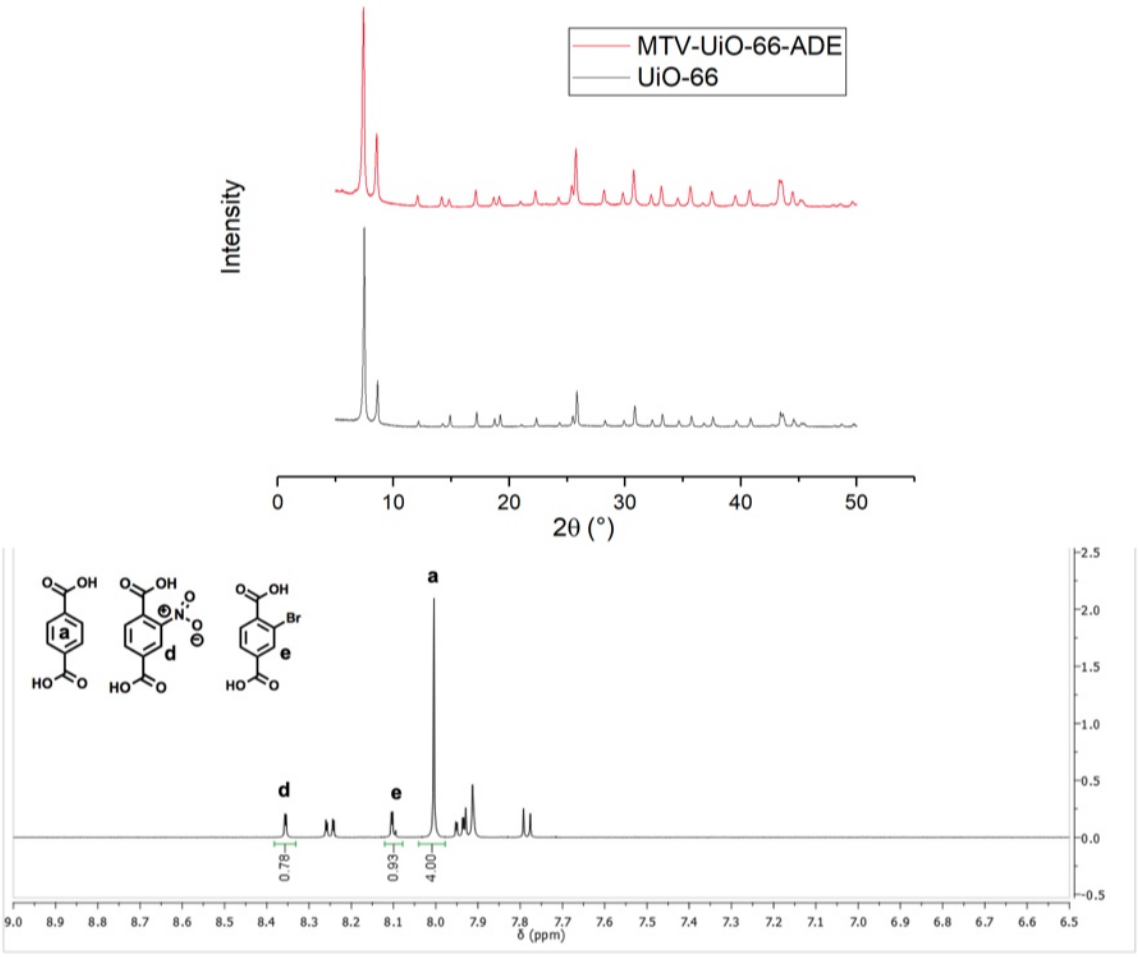

Figure S21. *Top*: PXRD of MTV-UiO-66-ADE. *Bottom*: ^{1}H NMR digestion of MTV-UiO-66-ADE.

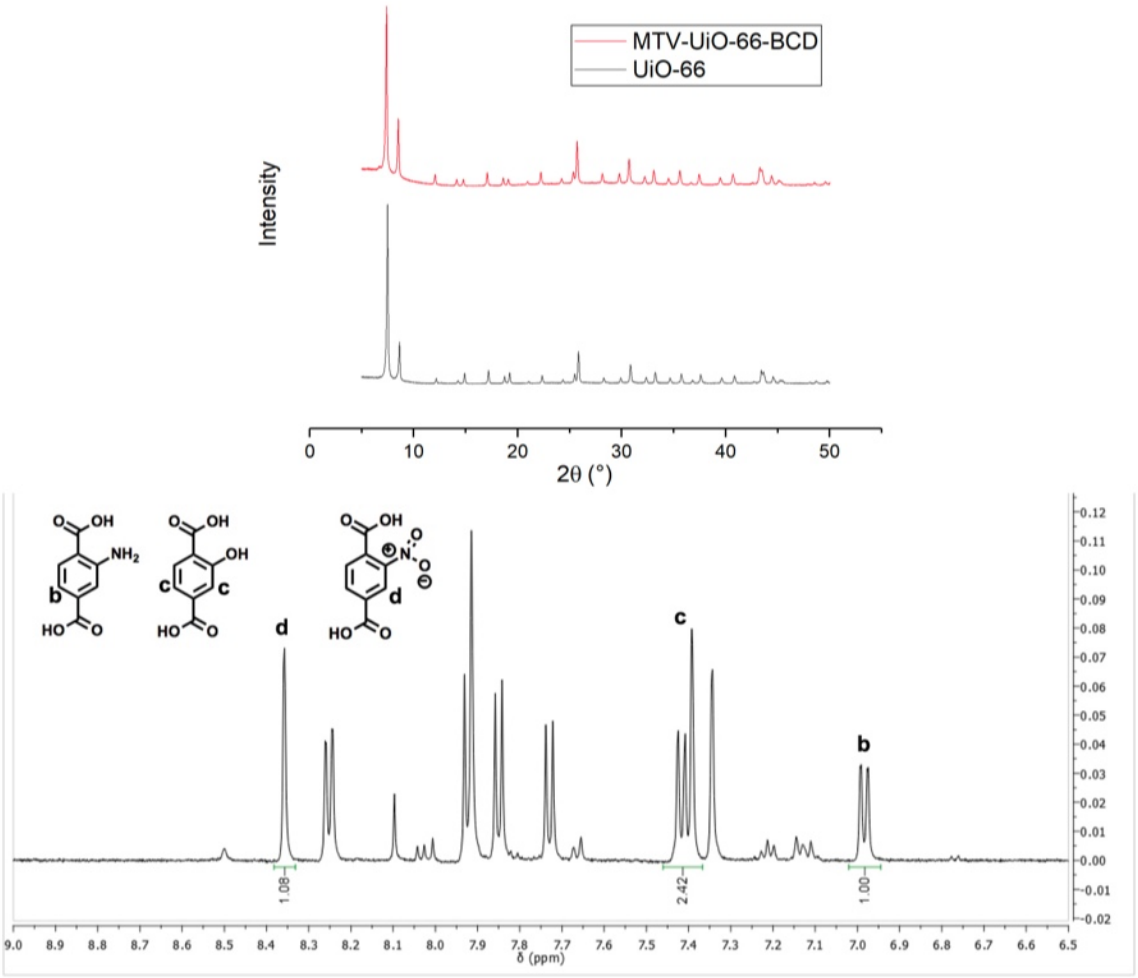

Figure S22. *Top*: PXRD of MTV-UiO-66-BCD. *Bottom*: ^{1}H NMR digestion of MTV-UiO-66-BCD.

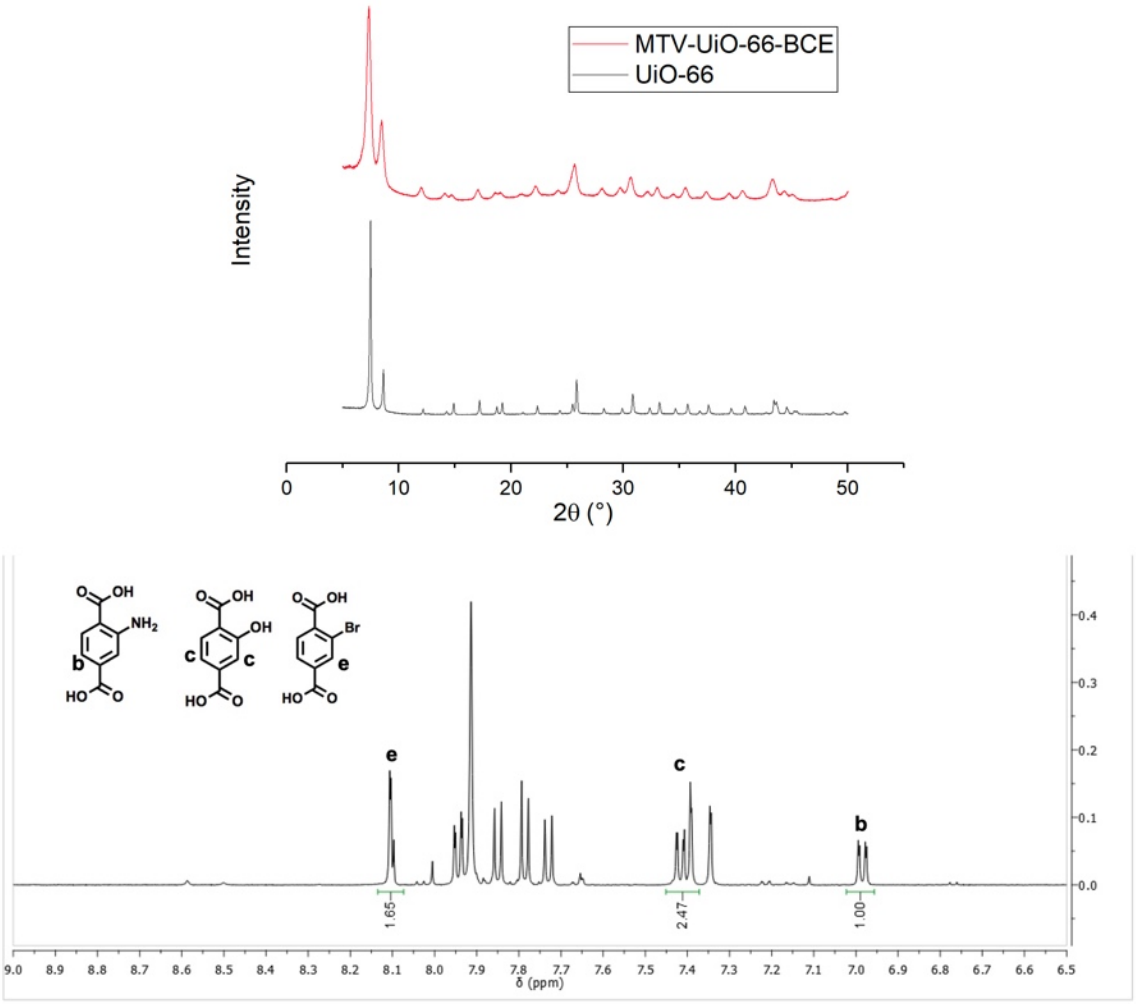

Figure S23. *Top*: PXRD of MTV-UiO-66-BCE. *Bottom*: ^{1}H NMR digestion of MTV-UiO-66-BCE.

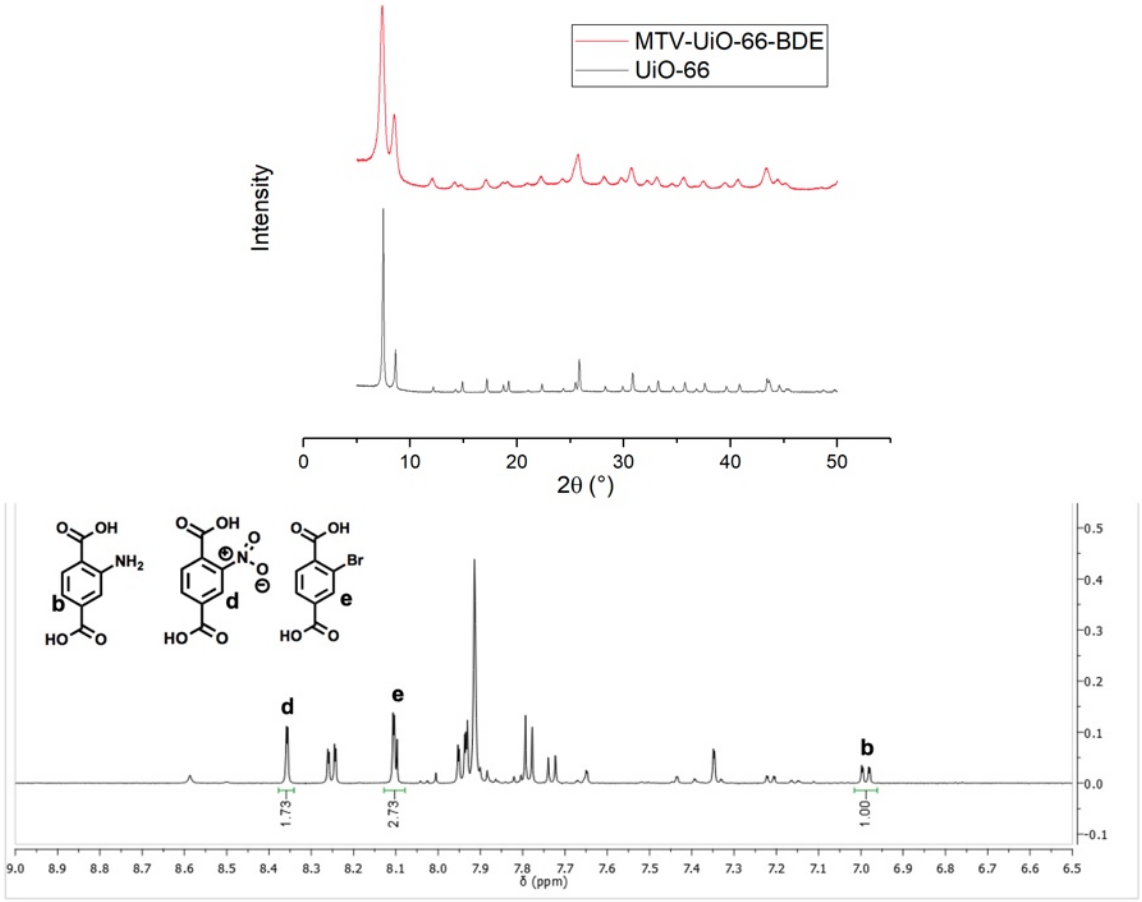

Figure S24. *Top*: PXRD of MTV-UiO-66-BDE. *Bottom*: ^{1}H NMR digestion of MTV-UiO-66-BDE.

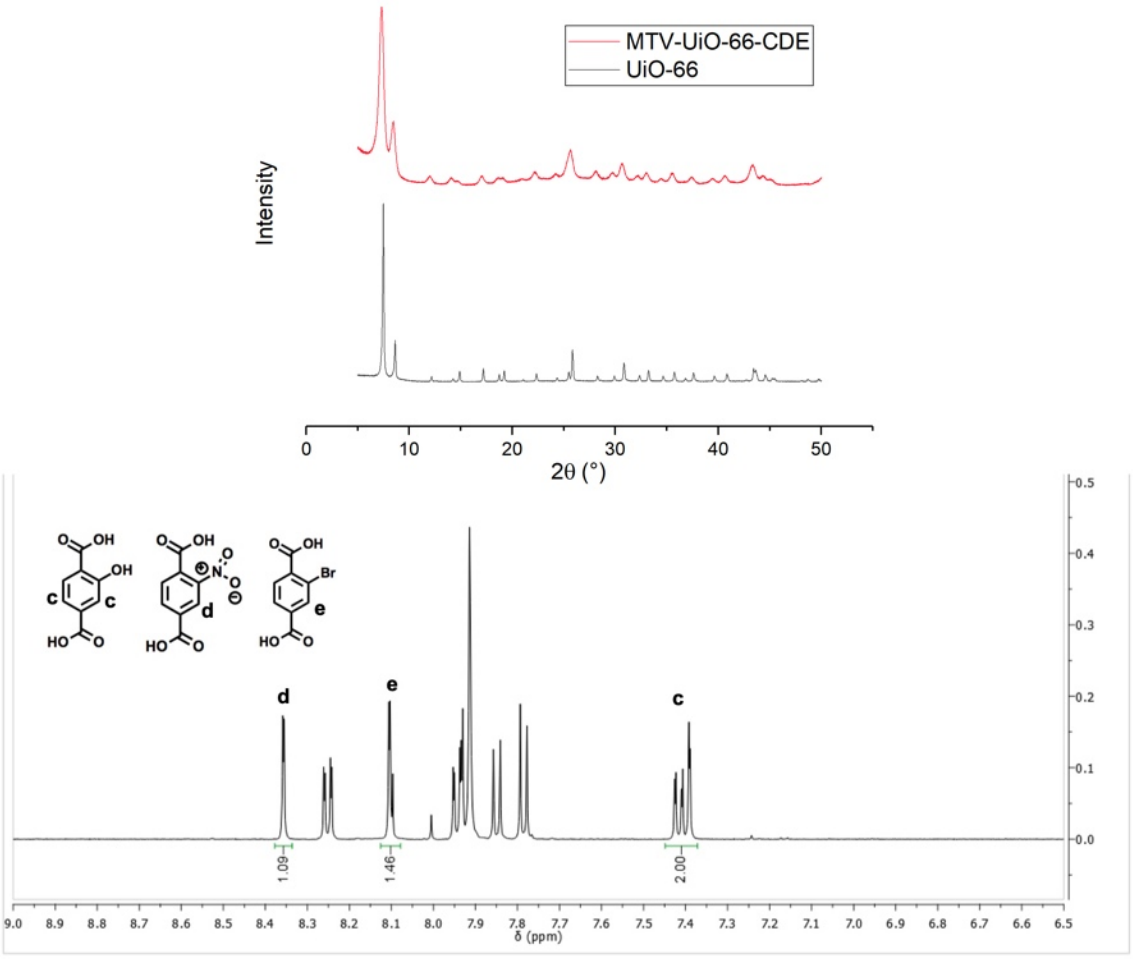

Figure S25. *Top*: PXRD of MTV-UiO-66-CDE. *Bottom*: ^{1}H NMR digestion of MTV-UiO-66-CDE.

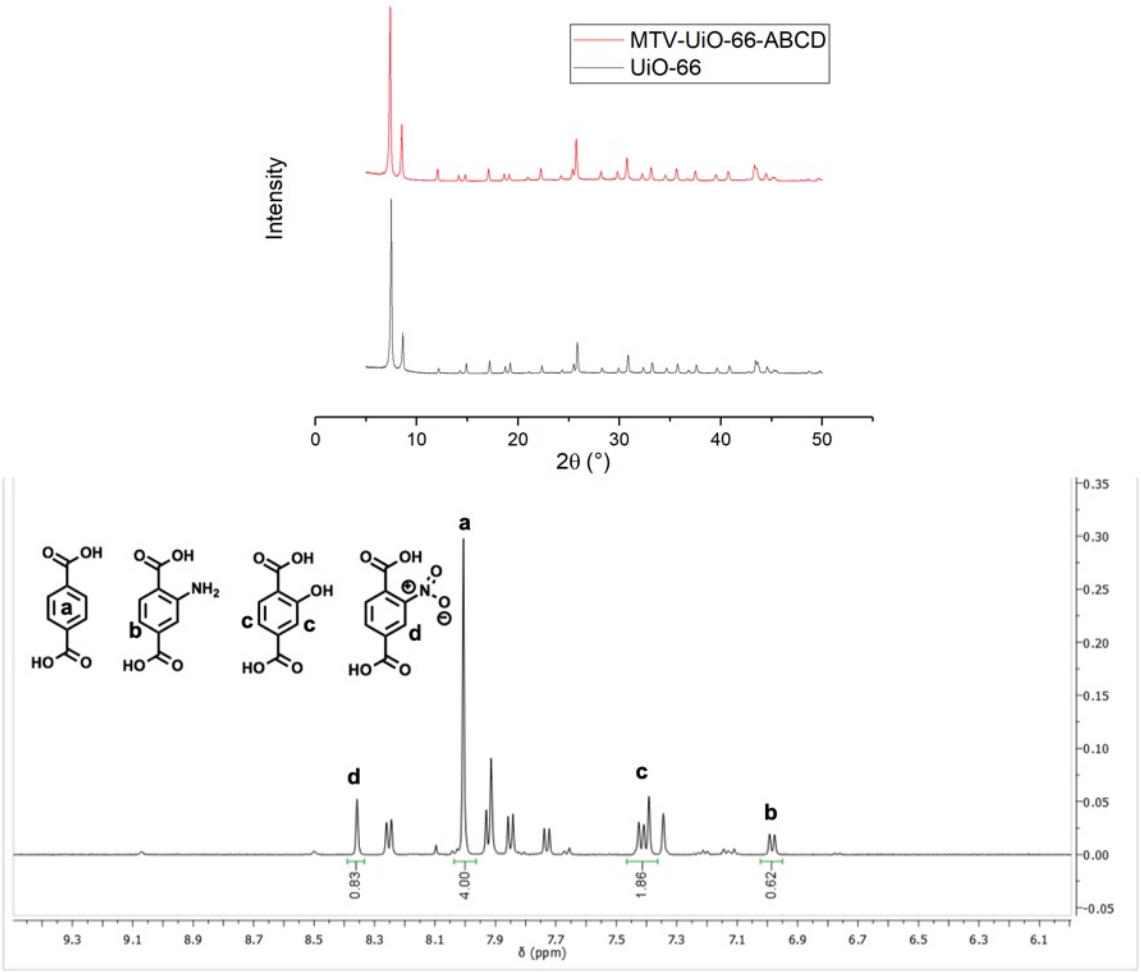

Figure S26. *Top*: PXRD of MTV-UiO-66-ABCD. *Bottom*: ^{1}H NMR digestion of MTV-UiO-66-ABCD.

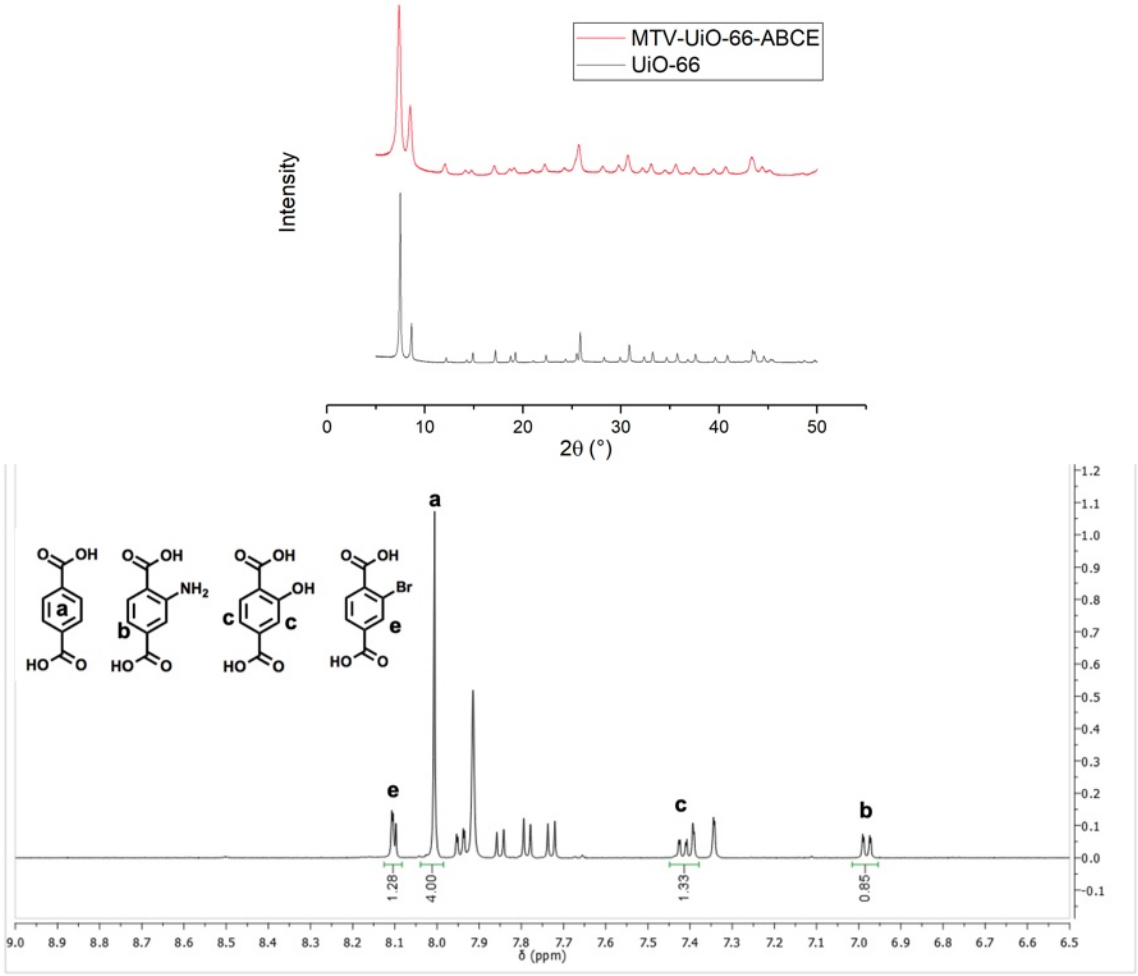

Figure S27. *Top*: PXRD of MTV-UiO-66-ABCE. *Bottom*: ^{1}H NMR digestion of MTV-UiO-66-ABCE.

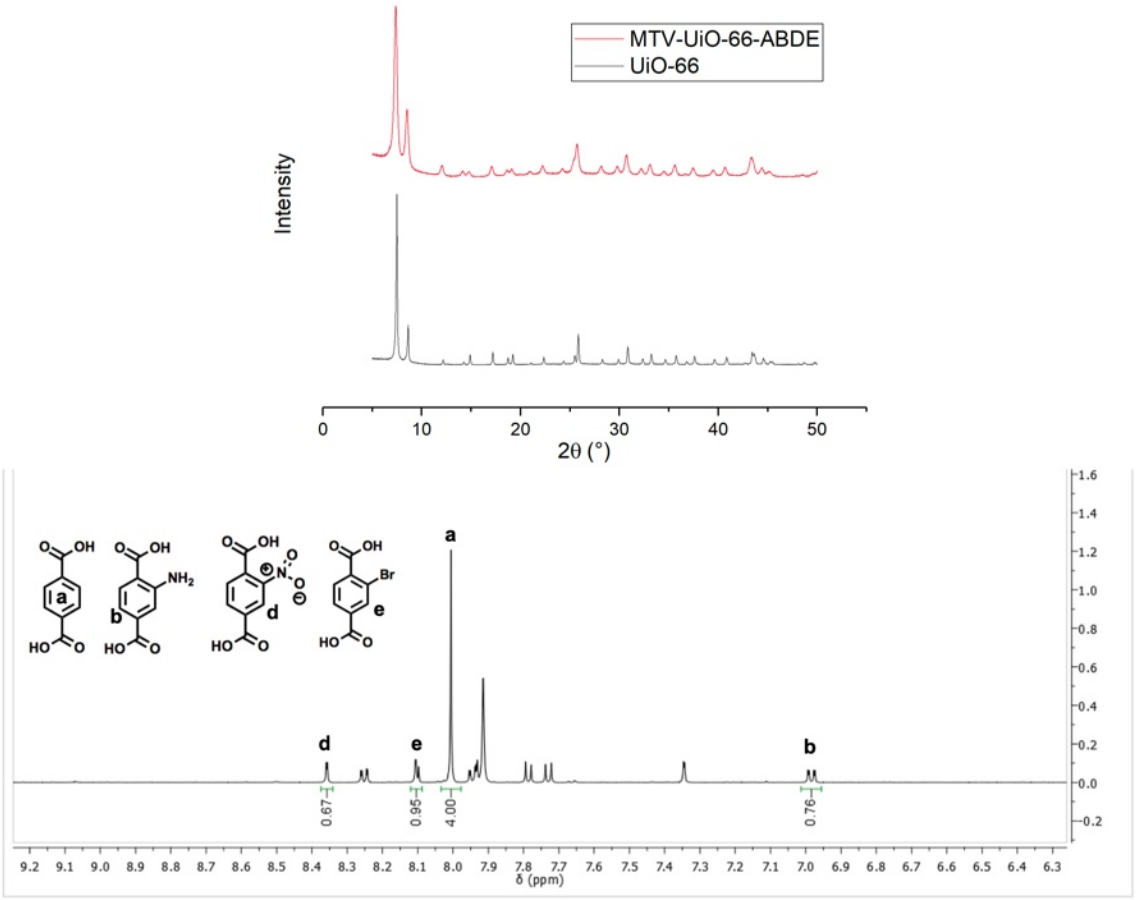

Figure S28. *Top*: PXRD of MTV-UiO-66-ABDE. *Bottom*: ^{1}H NMR digestion of MTV-UiO-66-ABDE.

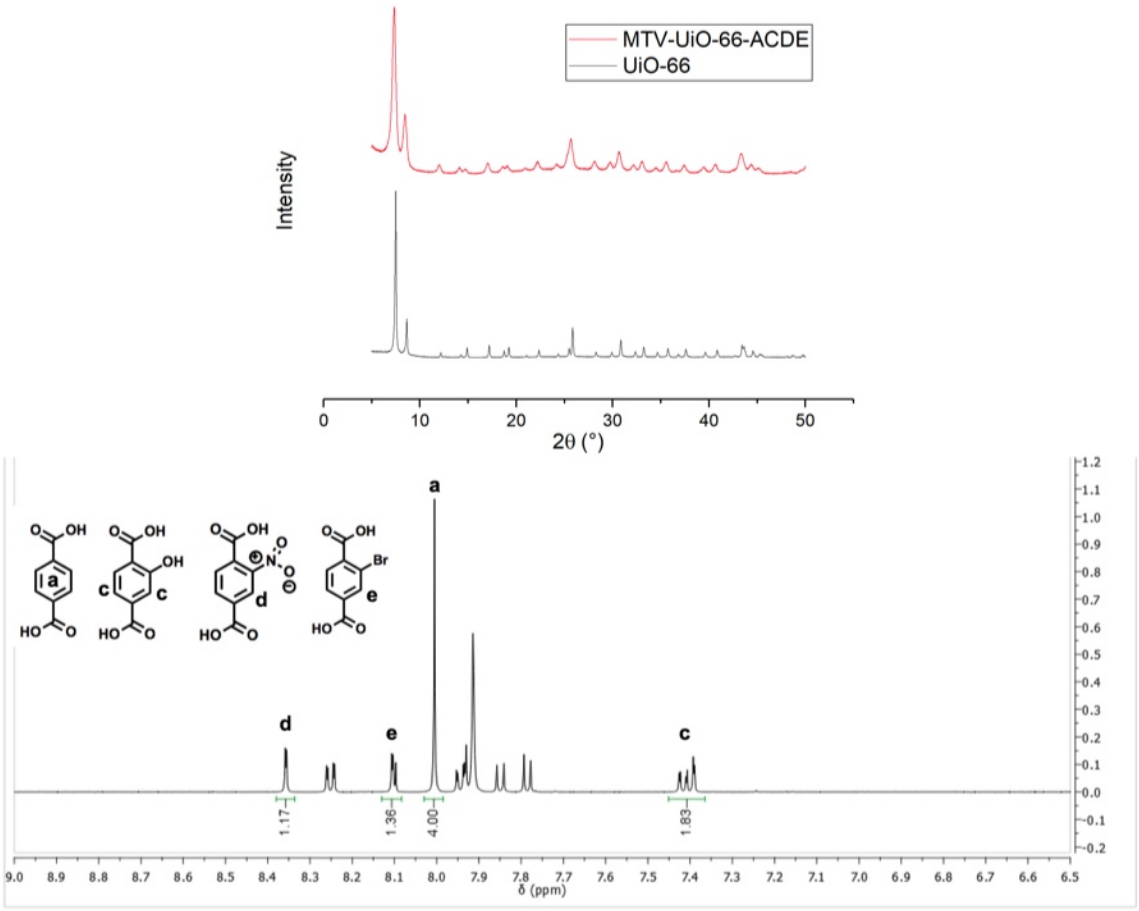

Figure S29. *Top*: PXRD of MTV-UiO-66-ACDE. *Bottom*: ^{1}H NMR digestion of MTV-UiO-66-ACDE.

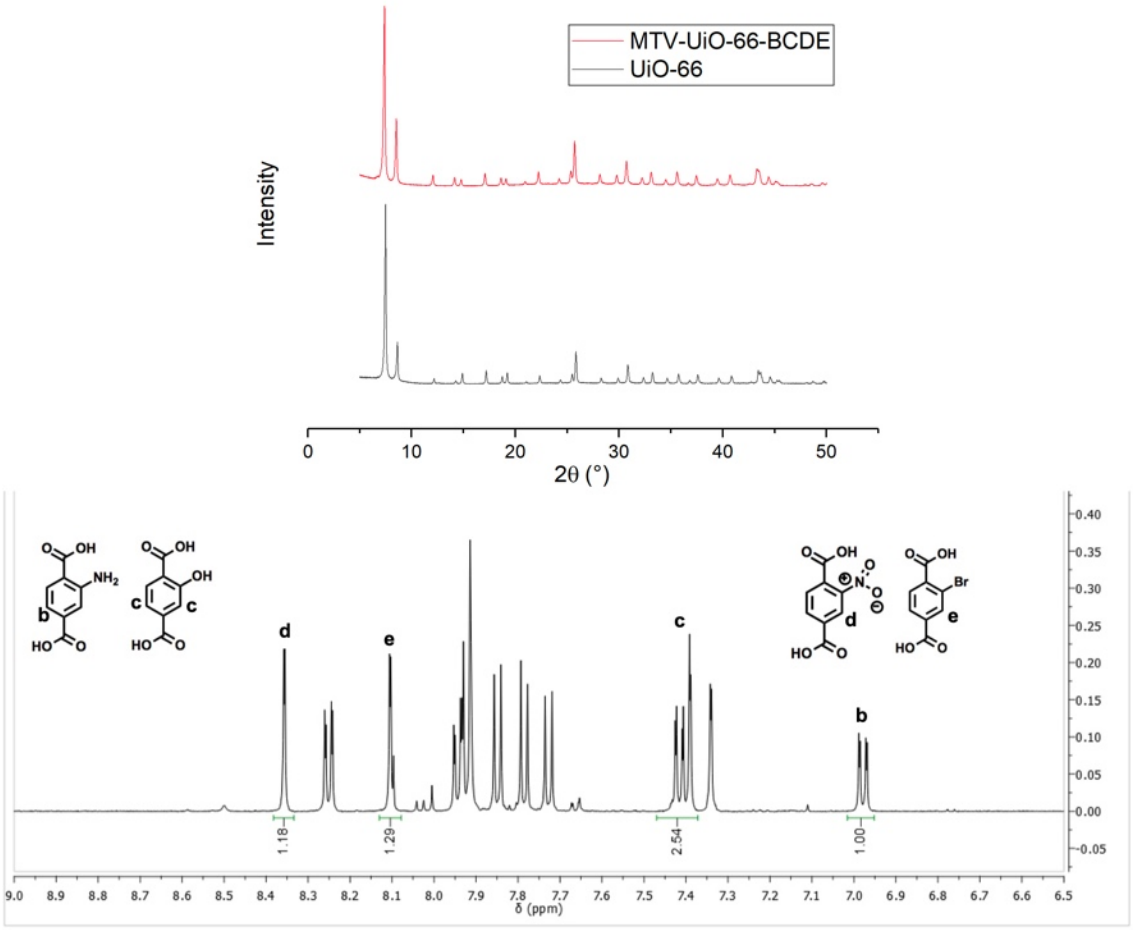

Figure S30. *Top*: PXRD of MTV-UiO-66-BCDE. *Bottom*: ^{1}H NMR digestion of MTV-UiO-66-BCDE.

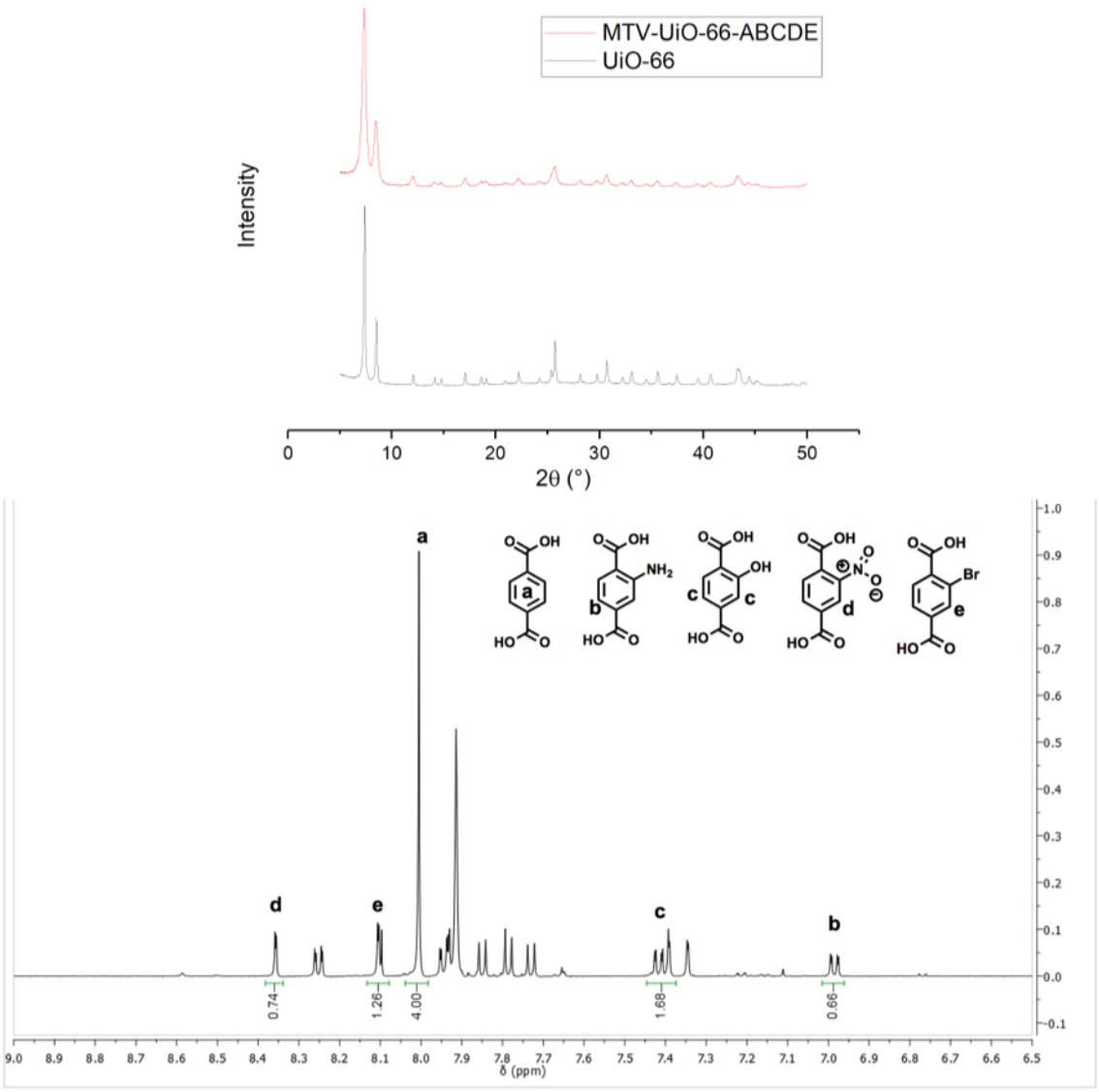

Figure S31. *Top*: PXRD of MTV-UiO-66-ABCDE. *Bottom*: ^{1}H NMR digestion of MTV-UiO-66-ABCDE.

Table S1. Ratio of MOF ligands determined by ^{1}H NMR and their respective stoichiometry in parentheses. The ratios are normalized to a value of one.

MTV-UiO-66 MOF	(A) BDC	(B) NH_2-BDC	(C) OH-BDC	(D) NO_2-BDC	(E) Br-BDC
A	1.00 (1)	N/A	N/A	N/A	N/A
B	N/A	1.00 (1)	N/A	N/A	N/A
C	N/A	N/A	1.00 (1)	N/A	N/A
D	N/A	N/A	N/A	1.00 (1)	N/A
E	N/A	N/A	N/A	N/A	1.00 (1)
AB	0.45 (1)	0.55 (1)	N/A	N/A	N/A
AC	0.50 (1)	N/A	0.50 (1)	N/A	N/A
AD	0.58 (1)	N/A	N/A	0.42 (1)	N/A
AE	0.49 (1)	N/A	N/A	N/A	0.51 (1)
BC	N/A	0.44 (1)	0.56 (1)	N/A	N/A
BD	N/A	0.49 (1)	N/A	0.51 (1)	N/A
BE	N/A	0.44 (1)	N/A	N/A	0.56 (1)
CD	N/A	N/A	0.50 (1)	0.50 (1)	N/A
CE	N/A	N/A	0.51 (1)	N/A	0.49 (1)
DE	N/A	N/A	N/A	0.48 (1)	0.52 (1)
ABC	0.36 (1)	0.30 (1)	0.34 (1)	N/A	N/A
ABD	0.38 (1)	0.28 (1)	N/A	0.34 (1)	N/A
ABE	0.40 (1)	0.23 (1)	N/A	N/A	0.37 (1)
ACD	0.36 (1)	N/A	0.33 (1)	0.31 (1)	N/A
ACE	0.34 (1)	N/A	0.34 (1)	N/A	0.32 (1)
ADE	0.37 (1)	N/A	N/A	0.29 (1)	0.34 (1)
BCD	N/A	0.30 (1)	0.37 (1)	0.33 (1)	N/A
BCE	N/A	0.26 (1)	0.32 (1)	N/A	0.42 (1)
BDE	N/A	0.18 (1)	N/A	0.32 (1)	0.50 (1)
CDE	N/A	N/A	0.28 (1)	0.31 (1)	0.41 (1)
ABCD	0.30 (1)	0.18 (1)	0.27 (1)	0.25 (1)	N/A
ABCE	0.26 (1)	0.22 (1)	0.18 (1)	N/A	0.34 (1)
ABDE	0.30 (1)	0.22 (1)	N/A	0.20 (1)	0.28 (1)
ACDE	0.23 (1)	N/A	0.21 (1)	0.26 (1)	0.30 (1)
BCDE	N/A	0.21 (1)	0.27 (1)	0.25 (1)	0.27 (1)
ABCDE	0.22 (1)	0.15 (1)	0.19 (1)	0.16 (1)	0.28 (1)

Scanning Electron Microscopy (SEM)

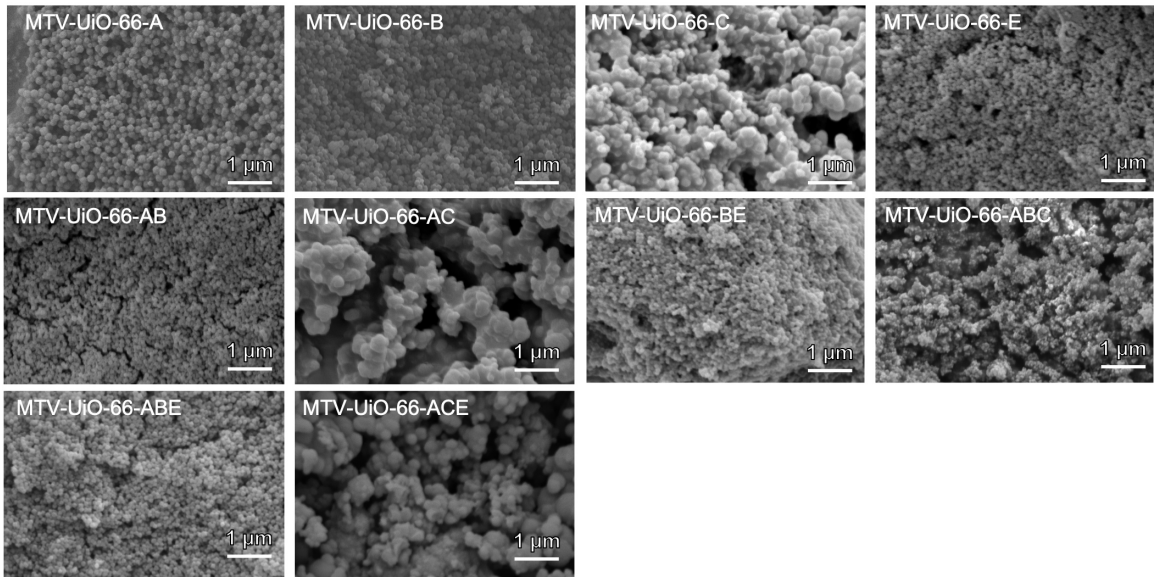

Figure 32. SEM images of MTV-UiO-66 MOFs.

N_2 Sorption Isotherms

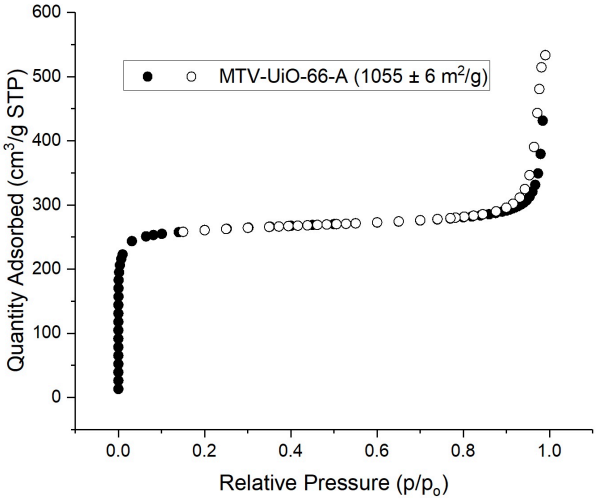

Figure S33. N_2 sorption isotherm for MTV-UiO-66-A.

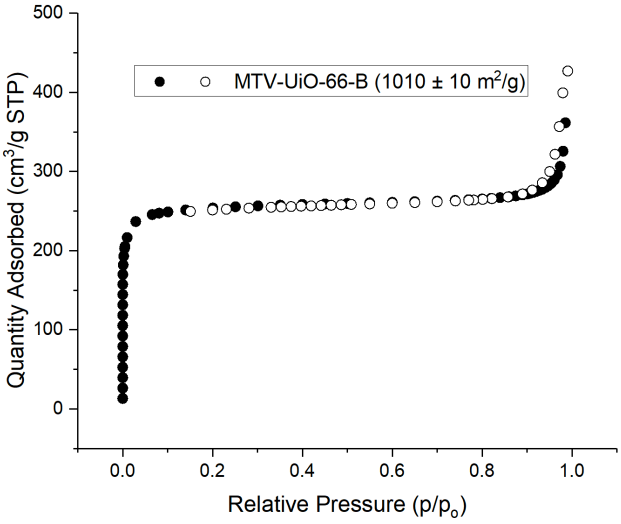

Figure S34. N_2 sorption isotherm for MTV-UiO-66-B.

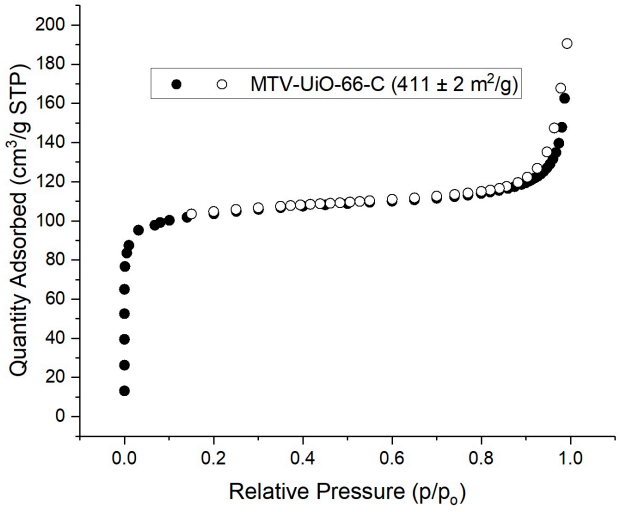

Figure S35. N_2 sorption isotherm for MTV-UiO-66-C.

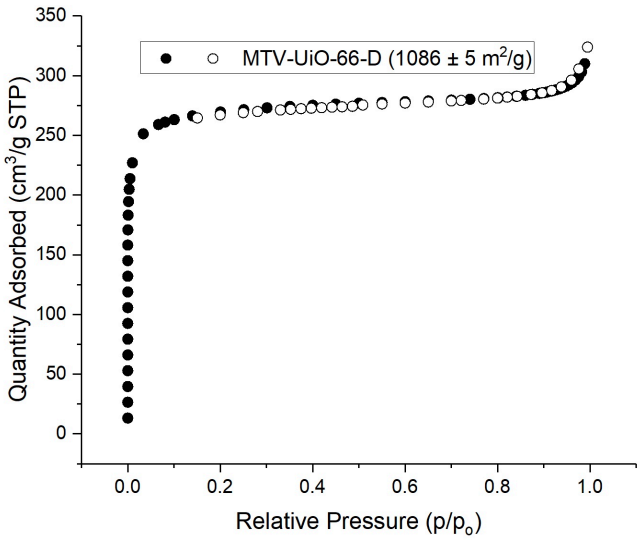

Figure S36. N_2 sorption isotherm for MTV-UiO-66-D.

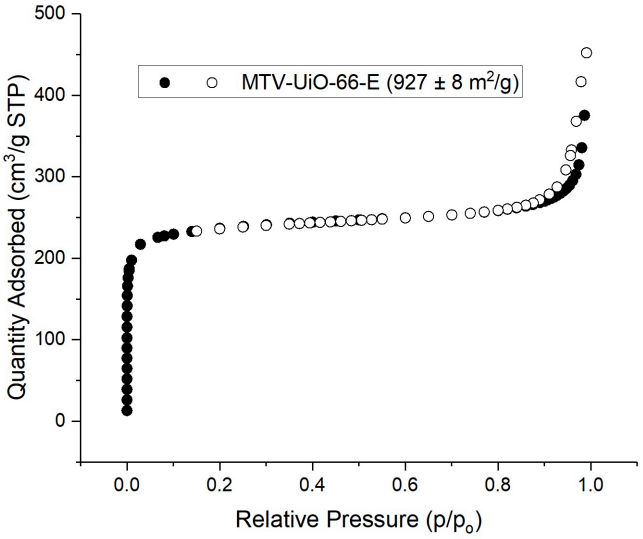

Figure S37. N_2 sorption isotherm for MTV-UiO-66-E.

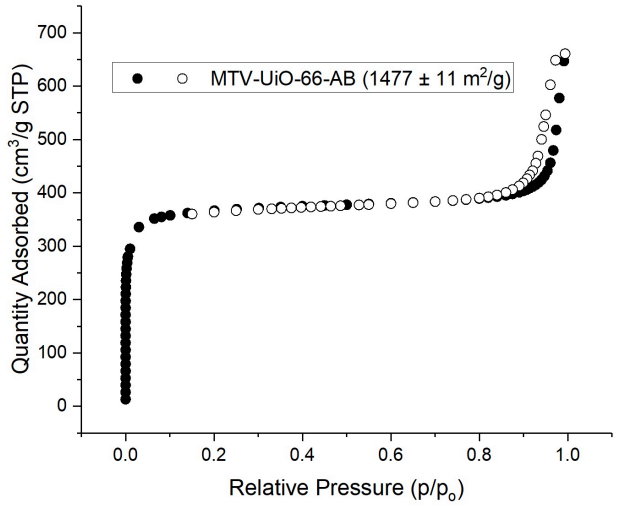

Figure S38. N_2 sorption isotherm for MTV-UiO-66-AB.

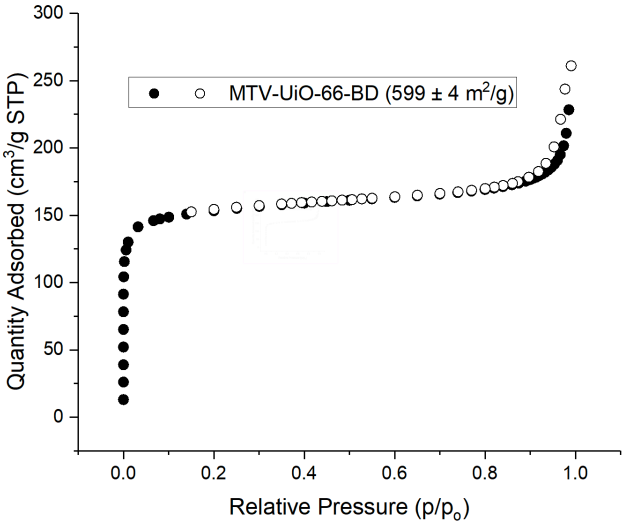

Figure S39. N_2 sorption isotherm for MTV-UiO-66-BD.

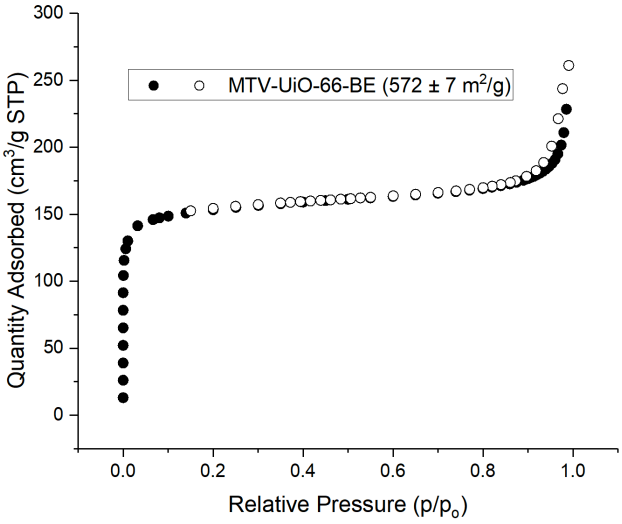

Figure S40. N_2 sorption isotherm for MTV-UiO-66-BE.

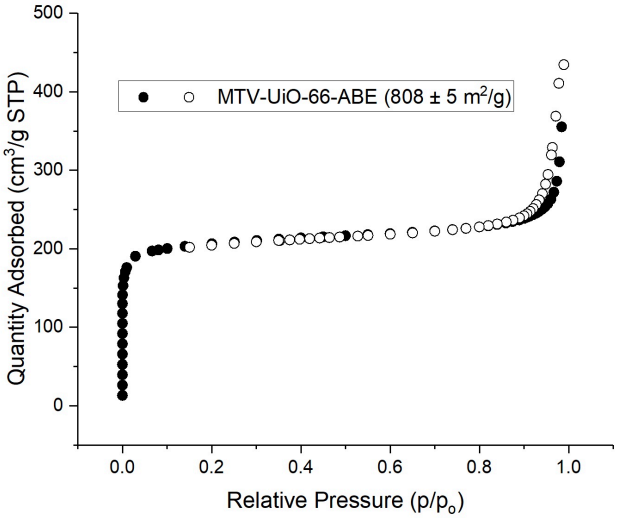

Figure S41. N_2 sorption isotherm for MTV-UiO-66-ABE.

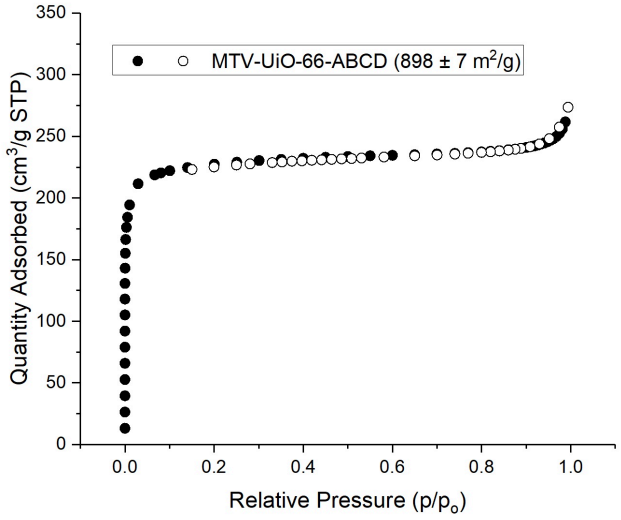

Figure S42. N_2 sorption isotherm for MTV-UiO-66-ABCD.

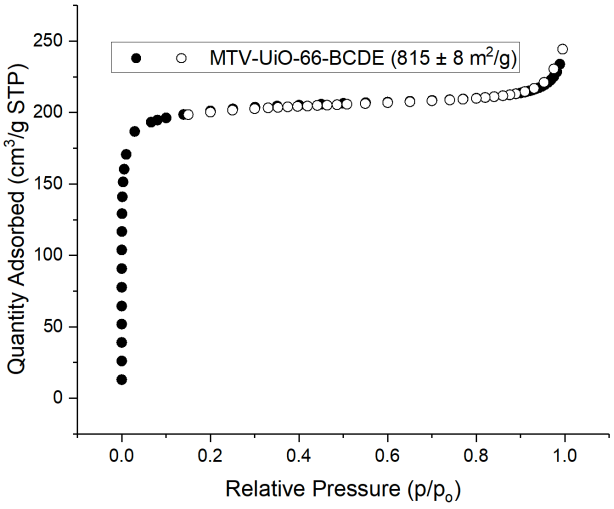

Figure S43. N_2 sorption isotherm for MTV-UiO-66-BCDE.

Thermogravimetric Analysis (TGA)

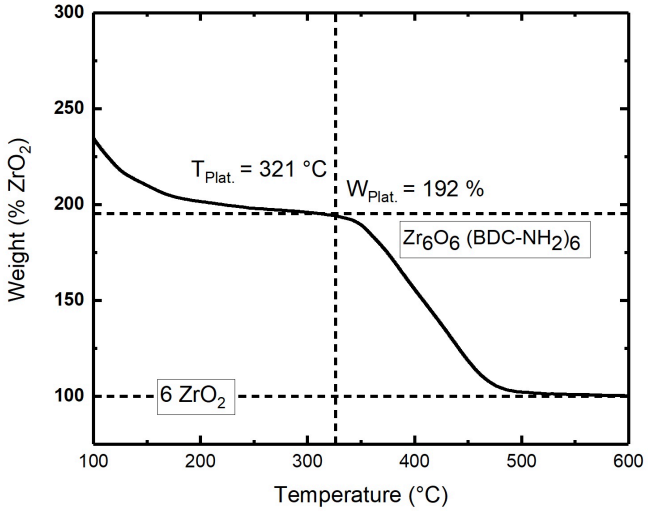

Figure S44. TGA trace for MTV-UiO-66-B.

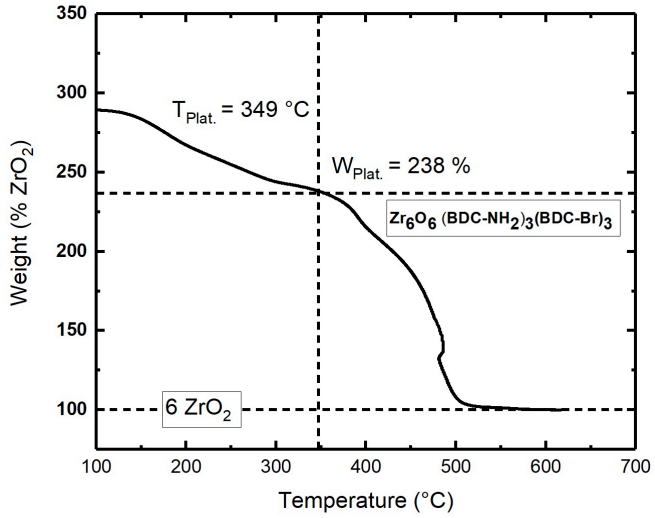

Figure S45. TGA trace for MTV-UiO-66-BE.

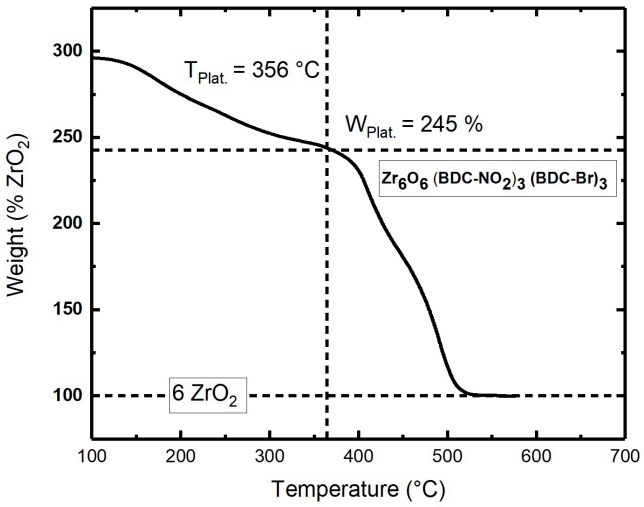

Figure S46. TGA trace for MTV-UiO-66-DE.

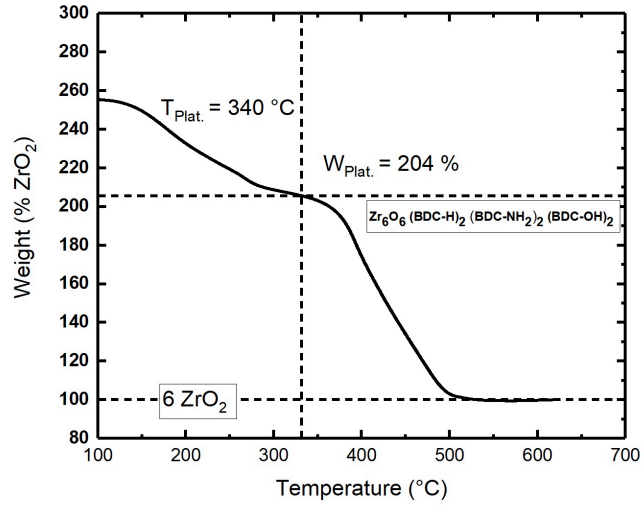

Figure S47. TGA trace for MTV-UiO-66-ABC.

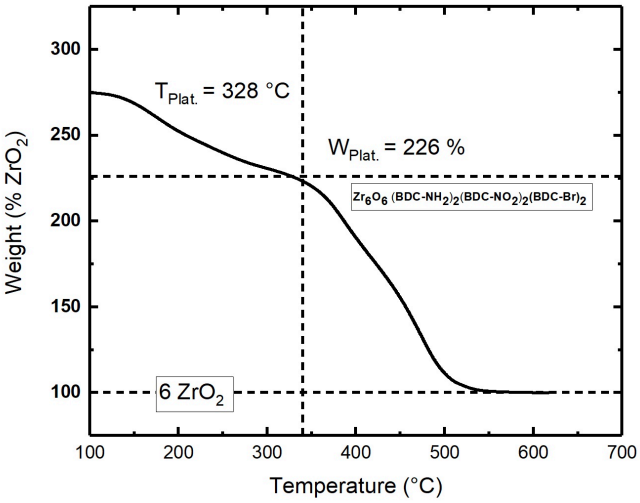

Figure S48. TGA trace for MTV-UiO-66-BDE.

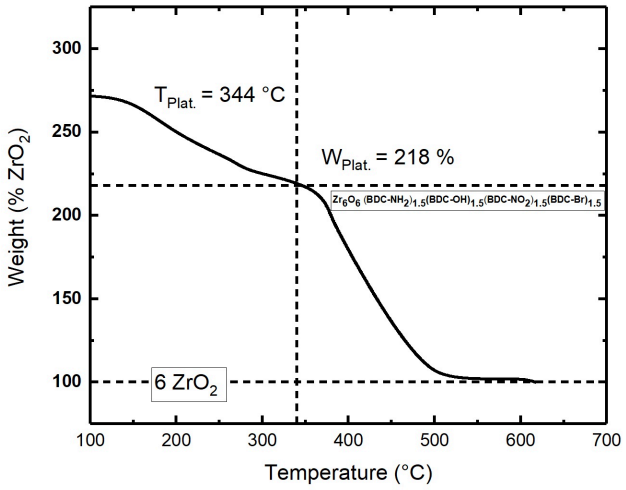

Figure S49. TGA trace for MTV-UiO-66-BCDE.

Table S2. MTV-UiO-66 MOF defects quantified as carboxylates per SBU.

MTV-UiO-66 MOF	**Carboxylates/SBU (12 = pristine)**
MTV-UiO-66-DE	9.4
MTV-UiO-66-B	10.2
MTV-UiO-66-BDE	9.2
MTV-UiO-66-ABC	8.4
MTV-UiO-66-BCDE	9.8
MTV-UiO-66-BE	10.4

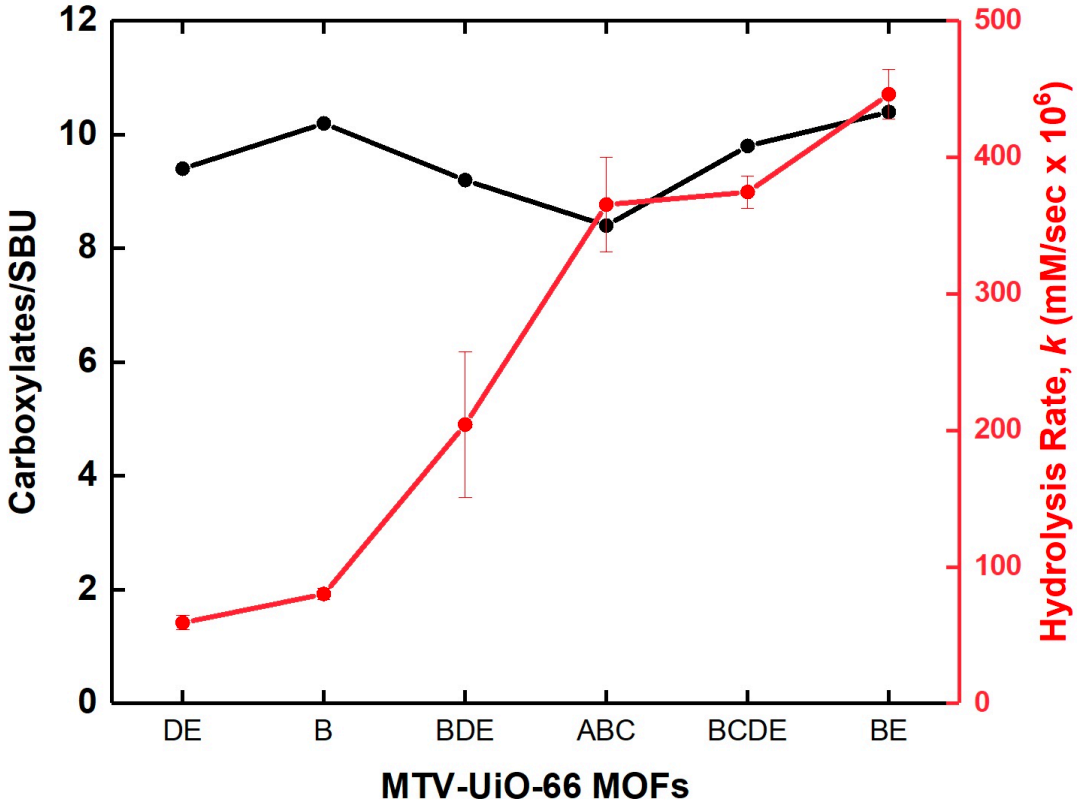

Figure S50. Ratio of organic linkers per SBU of MTV-UiO-66 MOFs (black) vs. rate of DMNP degradation by MOFs (red).